THE ENERGETIC PARTICLES: ACCELERATION, COMPOSITION, AND TRANSPORT (EPACT) INVESTIGATION ON THE WIND SPACECRAFT

T. T. VON ROSENVINGE, L. M. BARBIER, J. KARSCH, R. LIBERMAN, M. P. MADDEN, T. NOLAN, D. V. REAMES, L. RYAN, S. SINGH, H. TREXEL and G. WINKERT
NASA/Goddard Space Flight Center, Greenbelt, MD 20771, U.S.A.

and

G. M. MASON, D. C. HAMILTON and P. WALPOLE
Department of Physics, University of Maryland, U.S.A.

(Received 16 June, 1993)

Abstract. The Energetic Particles: Acceleration, Composition, and Transport (EPACT) investigation is designed to make comprehensive observations of solar, interplanetary, and galactic particles over wide ranges of charge, mass, energy, and intensity using a combination of 8 different particle telescopes. This paper summarizes the scientific goals of EPACT and provides a detailed description of the instrument design and capabilities.

Electrons are measured from 0.2 to 10 MeV, primarily providing time markers for injections of solar particles. Hydrogen is measured from 1.4 to 120 MeV, and Helium is measured from 0.04 to 500 MeV nucl^{-1}. The collection powers and energy ranges for heavier nuclei up to iron are ideal for observations of quiet-time populations such as particles accelerated by interplanetary shocks and the anomalous cosmic rays (thought to be accelerated at the boundary of the heliosphere). The large collection power available is also ideal for observations of ^{3}He, ^{4}He, and heavier nuclei in impulsive ^{3}He-rich solar events. There is even the possibility of observing ultra heavy nuclei ($Z > 30$) in large solar events for the first time. Finally, there is a telescope designed to measure isotopes from He (3.4–55 MeV nucl^{-1}) to Fe (12–230 MeV nucl^{-1}), which is intended for solar particles, the anomalous cosmic rays and galactic cosmic rays. The overall capabilities of EPACT provide scientifically interesting measurements over all phases of the solar cycle. There will also be important opportunities for combined studies with other spacecraft, such as SAMPEX, Ulysses, and Voyagers 1 and 2.

Table of Contents

Space Science Reviews **71:** 155–206, 1995.

1. Introduction

This paper describes the instruments which make up the Energetic Particles: Acceleration, Composition, and Transport investigation (EPACT) on the GGS/WIND spacecraft. These instruments are intended to be a major advance over their precursors on ISEE-3 and other spacecraft. These advances, described below, have come from improved detector technology, from higher density electronics, and from on-board microprocessors. Particle collection power has been increased by factors up to 100, while the telemetry bit-rate and allotted weight have only increased by factors of ~ 2. Improved detector technology permits larger collection areas and accurate trajectory determination. The latter is essential for resolving the individual isotopes of heavy nuclei.

We begin with a description of the scientific goals of EPACT and then devote the bulk of the paper to descriptions of each individual instrument. The on-board software, ground support equipment and system calibrations are also described.

2. Scientific Goals

The name of this investigation, Energetic Particles: Acceleration, Composition and Transport, enumerates our scientific goals. The acceleration of particles to high energies is ubiquitous throughout the solar system and beyond. We want to understand the various ways in which nature accomplishes this acceleration. The elemental and isotopic compositions of energetic particles are of intrinsic interest for what they tell us about source regions, but they also provide strong clues about how the particles are accelerated. The observations, generally from only a single point in space, often depend upon, among other things, poorly known boundary conditions. For example, the way particles are transported from their sources to us can be very difficult to infer. At the same time, correct interpretation of our observations may depend upon knowing these boundary conditions. Extensive models of particle transport have been evolving over the last two decades. We hope to test these models with observations. Combining EPACT data with data from

Ulysses while it is over the solar poles may also shed light on particle transport in the heliosphere.

Particle populations whose acceleration, composition and transport are of central interest include particles from solar events, particles accelerated in situ by interplanetary shocks, the so-called anomalous component, and galactic cosmic rays. Typical differential intensity spectra are illustrated in Figure 2-1. We briefly discuss each in turn. The launch of the WIND spacecraft in 1994 will initially emphasize quiet-time studies as opposed to solar events.

2.1. SOLAR ENERGETIC PARTICLE EVENTS

Major progress has been made in the last decade by members of the EPACT team in understanding solar energetic particles. This progress was based on data from earlier instruments on IMP-8 and ISEE-3 (for example, see review by Reames, 1990). Briefly, two event classes, impulsive and long duration, have been recognized as arising from acceleration at an initial event site and from acceleration due to a shock wave emanating from the event site, respectively. The shock wave may continue to accelerate particles all the way from the solar corona to beyond 1 AU. Impulsive events are associated with the acceleration of electrons, Type III radio emissions, and, frequently, large enhancements of both ^{3}He and heavy nuclei. The causes of these enhancements are just beginning to be understood, but it is apparent that preferential acceleration of the ions occurs because of selective absorption of plasma waves generated by the streaming electrons (Temerin and Roth, 1992; Miller and Viñas, 1993). Long duration events typically reflect the composition of the corona and show compositional differences relative to the solar photosphere which have a clear dependence on first ionization potential (FIP). Unlike impulsive events, they are dominated by energetic protons and are highly correlated with Coronal Mass Ejections (CMEs). The CMEs drive the shock waves which then accelerate particles out of the ambient plasma. As might be expected from this picture, impulsive events are seen near Earth only when they occur in regions magnetically well-connected to Earth, whereas long duration events can be observed from a broad range of solar longitudes.

Previous studies of heavy nuclei from the Sun have suffered from limited collection power and hence poor statistics. EPACT will have up to 100 times greater collection power and hence should be able to make much more sensitive observations of, for example, event to event variations of composition. ^{3}He-rich events are invariably associated with low-energy electrons, but the inverse is not true: there are 5 to 10 times as many electron events observed as there are ^{3}He-rich events. We do not presently know whether this is because we have had inadequate sensitivity to ^{3}He or whether some electron events are fundamentally different from those accompanying ^{3}He-rich events. Such studies will be undertaken in concert with electron measurements from the 3-D Plasma/Energetic Particle Investigation on WIND. With its large collecting power, EPACT also has the possibility of

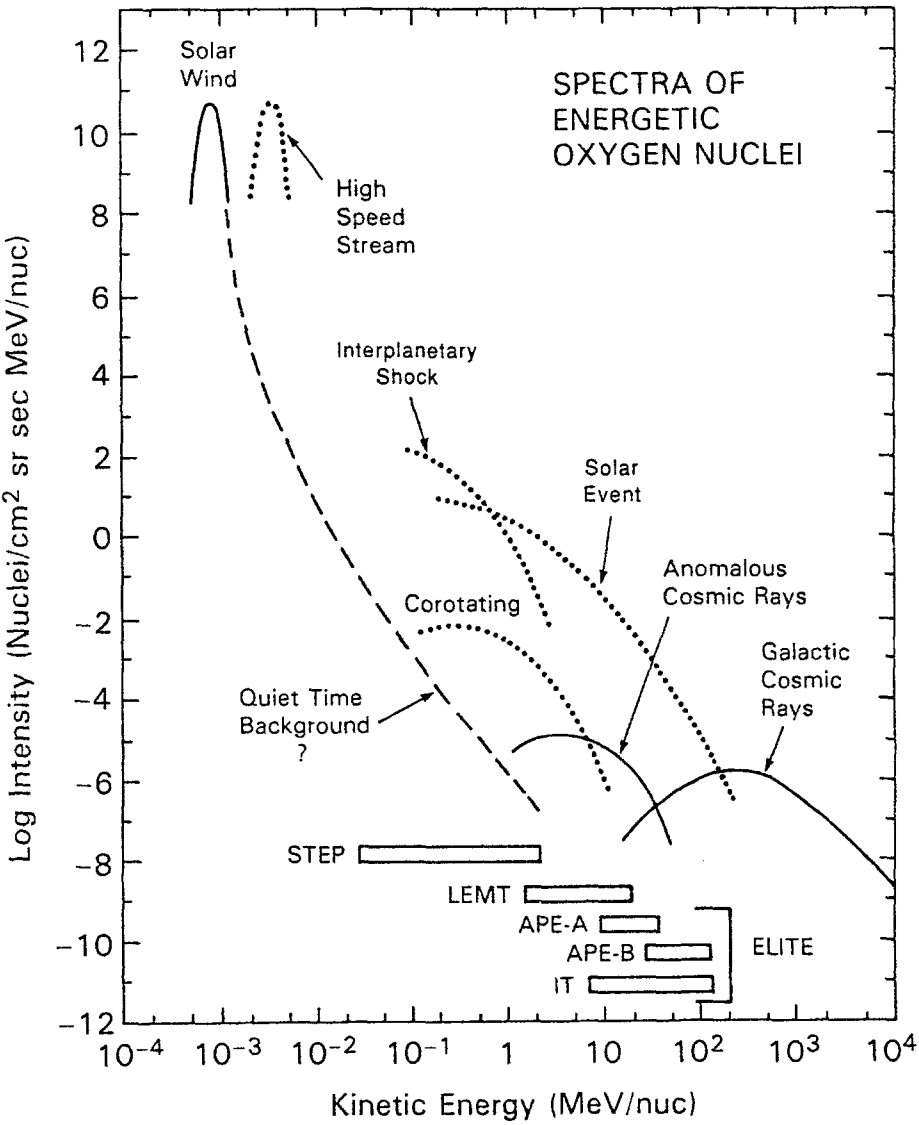

Fig. 2-1. Typical oxygen spectra for different populations of interplanetary particles. The energy ranges for each EPACT telescope are also shown.

making the first observations of solar particles considerably heavier than iron. Enhancements of heavy nuclei are sometimes seen to increase for increasingly heavy elements up through iron. It is not yet known if these enhancements persist to even heavier elements. We also plan to compare our abundance data with abundances derived from gamma-ray lines observed by the Transient Gamma Ray Spectrometer (TGRS) instrument on WIND. Finally, the Isotope Telescope will

look for isotope anomalies similar to the enrichment of $^3He/^4He$, in part to shed further light on the acceleration process.

2.2. INTERPLANETARY SHOCKS

Interplanetary shocks include both transient shocks generated by CMEs and also longer lived shocks associated with high speed streams in the solar wind overtaking low speed streams, forming so-called Corotating Interaction Regions (CIRs). For transient shocks, it is possible to make observations upstream and downstream of the shocks as they go past the spacecraft and hence to see acceleration taking place *in situ*. The FIP effect for ions accelerated from the high-speed solar wind in CIRs appears to be different than for solar events (Reames *et al.*, 1991), indicating differences in the FIP fractionation process beneath coronal holes. Poor statistics have been a limiting factor in previous studies of CIR composition. The STEP energy range is particularly well-suited to exploring CIRs. Upstream particles from the Earth's bow shock will also be studied by STEP. Their composition can indicate whether they have been accelerated out of the solar wind or originate from some region inside the magnetosphere.

2.3. ANOMALOUS COMPONENT

The anomalous component is thought to be a sample of the nearby interstellar medium which is accelerated at the solar wind termination shock. The Isotope Telescope was specifically designed to cover the energy range required to study the isotopic composition of the anomalous component and hence of the contemporaneous interstellar medium. With our greatly increased collection power, we will also be able to greatly improve the study of time variations of this very low intensity population. EPACT observations outside the Earth's magnetosphere will be compared with data taken inside the magnetosphere by the Solar, Anomalous and Magnetospheric Particle Explorer (SAMPEX). The transport and solar modulation of the anomalous component within the solar system are also of considerable interest, so we will compare intensities measured by Ulysses while it is over the solar poles with values observed in the ecliptic by EPACT.

2.4. GALACTIC COSMIC RAYS

Galactic cosmic rays are the only direct sample of matter originating from beyond the solar system. It is perhaps surprising, then, that their source composition is remarkably similar to the composition of the solar corona (as reflected by the composition of long-duration solar events). For example, the galactic cosmic rays display a similar FIP effect in their abundances. On the other hand there are well known differences in the isotopic composition. For example, there is much more ^{22}Ne in the galactic cosmic ray source relative to ^{20}Ne than in the solar system. These differences are just beginning to be explored.

The lifetime of the galactic cosmic rays has been measured to be 10 million years using the radioactive clock ^{10}Be (for example, see the review by Simpson and Garcia-Munoz, 1988). Other radioactive clocks such as ^{26}Al, ^{36}Cl, ^{54}Mn, and ^{59}Co have also just begun to be explored.

3. Instrument Hardware

3.1. Overview

The EPACT investigation must make measurements over an extremely broad range of elements, energies and intensities. As a result, EPACT consists of multiple telescopes that also provide a level of protection against single-point failures. An early configuration consisted of two independent systems, the *L*ow *E*nergy *M*atrix *T*elescope system (LEMT) and the *El*ectron-*I*sotope *Te*lescope system (ELITE). Each of these two systems has three solid-state detector telescopes with a common Data Processor Unit design. LEMT contains three identical LEMT telescopes, whereas ELITE contains two Alpha-Proton-Electron (APE) telescopes and an Isotope Telescope (IT). LEMT and ELITE have been designed, built and tested by the Low Energy Cosmic Ray Group and the Electronics Systems Branch of the Laboratory for High Energy Astrophysics at the NASA/Goddard Space Flight Center. Subsequently, the *S*upra*t*hermal *E*nergetic *P*article telescope system (STEP) was added to EPACT. STEP, which contains two identical telescopes, is interfaced to the spacecraft through ELITE. STEP was originally designed and partially built by the University of Maryland for the U.S. ISPM spacecraft which was cancelled in 1980. The University of Maryland completed the construction and testing of STEP for EPACT.

All the telescopes except for those in STEP use the $\mathrm{d}E/\mathrm{d}x$ by E method of particle identification. Solid-state detectors are used throughout for reliability and long-term gain stability. STEP measures time-of-flight and energy, from which particle mass can also be obtained. Each STEP telescope includes a start and stop microchannel plate detector as well as a solid-state detector to measure the total energy. Salient characteristics of these telescopes are presented in Table I.

The mounting of LEMT, ELITE and STEP on the WIND spacecraft is illustrated in Figure 3.1-1. The spacecraft $+X$-axis points along the magnetometer boom, the $+Z$-axis points to the top of the spacecraft, and the $+Y$-axis completes a right-handed coordinate system. In flight, the spacecraft $+Z$-axis will be pointing towards the south-ecliptic pole and the spacecraft will be spinning with a nominal spin period of 3 s. The look directions of the three LEMT telescopes combined with the spin of the spacecraft permit near omnidirectional viewing (Telescope A is canted 25° below the spacecraft $X-Y$ plane, Telescope B looks directly into the $X-Y$ plane, and Telescope C is canted 25° above the $X-Y$ plane). One of the STEP telescopes views 26° above the ecliptic and one 26° below, thus eliminating

TABLE I
EPACT telescope summary

	LEMT	APE-A	APE-B	IT	STEP
Charge range	2 to 90	−1 to 26	−1 to 26	2 to 26	2 to 26
Energy range					
Electrons (MeV)	–	0.2–2	1–10	–	–
Hydrogen (MeV)	1.4–10	4.6–25	19–120	–	–
Helium (MeV nucl^{-1})	1.4–10	4.6–25	19–500	3.4–55	0.04–8.1
Iron (MeV nucl^{-1})	2.5–50	15–98	73–300	12–230	0.020–1.2
Geometry factor (cm^2 sr)	3 × 17	1.2	1.3	~ 9.0	2 × 0.4

TABLE II
EPACT resource allocations

System	Weight (kg)	Power (W)	Bit-rate (bits s^{-1})
LEMT	14.6	8.82	206
ELITE	12.7	8.65	205
STEP	3.1	3.08	63
Totals	30.4	20.55	474

direct solar UV from the fields of view (nominally 17° × 44°). Commandable doors across the two entrance apertures of STEP protect very thin (~ 1000 Å) foils from vibration during launch and provide additional Sun-shading after they are opened. The remaining telescopes look into the ecliptic plane. The APE-B telescope is mounted as far out from the side of the spacecraft as possible and in such a way that the forward look angle is unobstructed and the backward look angle is nearly so.

The weight, power and telemetry resources required by each system are summarized in Table II. The LEMT and ELITE weights were allowed to be higher than initially planned in order to reduce cost. The bit-rates are given for the predominant spacecraft telemetry rate of 92 s/Major Frame.

Several elements which are used in common by the different systems will be described briefly here.

Pulse-height analysis for LEMT and ELITE is performed using 16-bit analog-to-digital converters (ADCs, model CS5016TD16M) manufactured by Crystal Semiconductor Corporation. These successive-approximation chips complete a

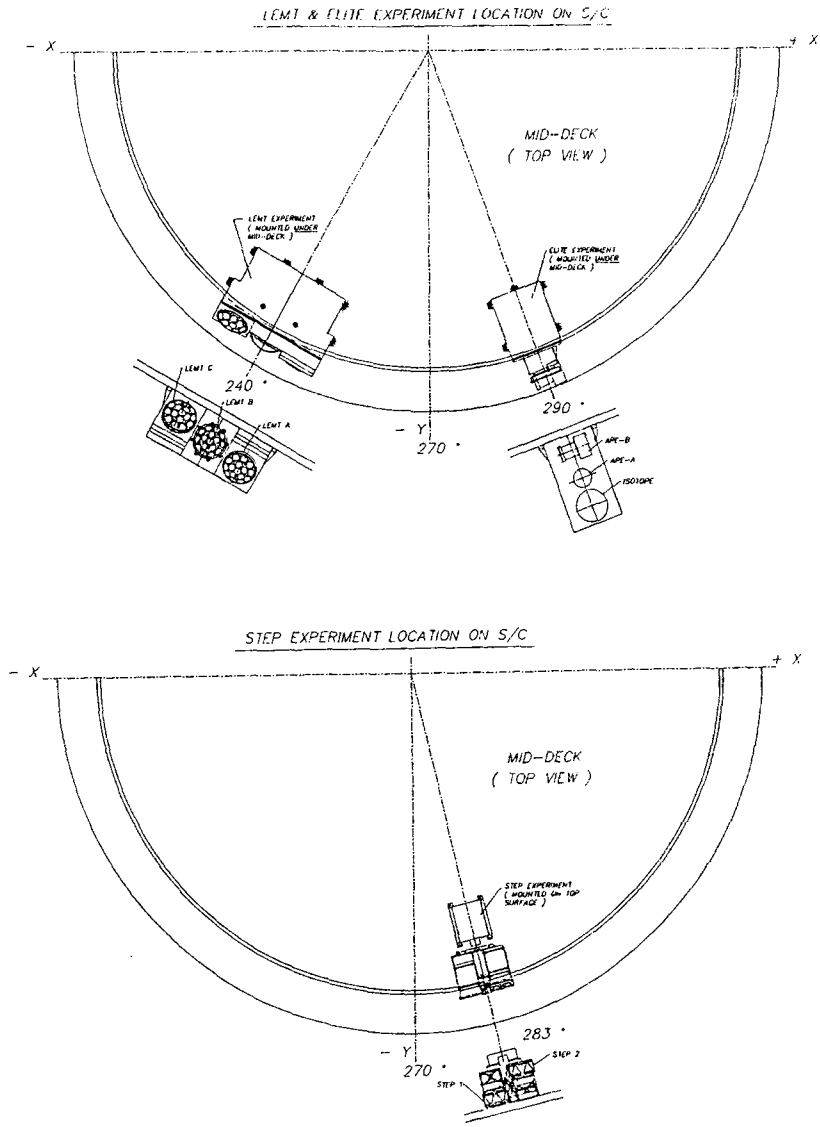

Fig. 3.1-1. Shows the mounting locations of LEMT, ELITE and STEP on the WIND spacecraft.

conversion in approximately 20 μs. Baseline offsets are measured periodically by each system. These offsets are used by the on-board particle analysis algorithms and are also reported to the ground via telemetry. The ADC chip is subject to possible latchup if a highly ionizing particle passes through the chip. A power control circuit switches off the ADC in the event that a latchup (excessive current) condition is detected. Subsequent turn-on of the ADC under microprocessor control returns it to normal operation.

Two semi-custom gate-array chips were developed for EPACT (Winkert, 1992). One, a programmmable counter chip, has 16 24-bit counters for counting hardware rates. Ten such chips are used by EPACT. The second is for holding the states of command bits which are either sent to EPACT by ground command or are established by on-board software.

Another EPACT innovation is the use of Random Access Memory (RAM) chips to perform coincidence logic. Two- (or three-dimensional) pulse height space can be subdivided into rectangular areas (or volumes) by threshold discriminator levels associated with each of the signal axes. By judicious choices of discriminator levels, combinations of these areas (or volumes) can be made to separately enclose, for example, electrons, protons, helium and heavier nuclei in different energy intervals. The states of the discriminator levels on each axis are encoded and applied to the address lines of the coincidence RAM. For example, if there are 8 different discriminator levels on one axis then the highest level fired is encoded and latched into three bits. Other logic levels such as an anti-coincidence threshold or mode bits coming from a central microprocessor can also be applied to the address lines. The RAM chip is strobed by a simple coincidence from, let's say, the front two detectors in a telescope. The strobe causes readout of an 8 bit memory value from the RAM. One bit of this memory value determines whether events of this type are pulse-height analyzed in the current mode. Another four bits might be used to encode which of 16 different hardware rate counters is to be incremented. For example, these rate counters might correspond to electrons, protons, helium and heavier nuclei in different energy intervals. The coincidence RAM contents on EPACT are uploadable by ground command. This permits relaxing of coincidence requirements during testing as well as altering the coincidence logic after launch.

The spacecraft design specifications permit the spacecraft to exceed 35° C, a temperature which the surface barrier detectors and microchannel plates in EPACT cannot exceed. The EPACT telescopes are therefore, to a large degree, thermally isolated from the spacecraft and their electronics, allowing them to run cooler than the spacecraft during normal flight conditions. During the mission, however, solar eclipses will occur due to both the Earth and the moon, with the longest being as long as 90 min. Thermostatically controlled survival heaters are enabled for these periods of spacecraft shadow. The thermostats are necessary to prevent over-heating during non-shadow periods. The instrument electronics are turned off to provide the necessary heater power. During a shadow the electronics will not cool excessively since they are bolted to a large heat reservoir (i.e., the spacecraft), whereas, without the heaters, the low-mass telescopes would get very cold when their major source of heat input (incident sunlight) disappears.

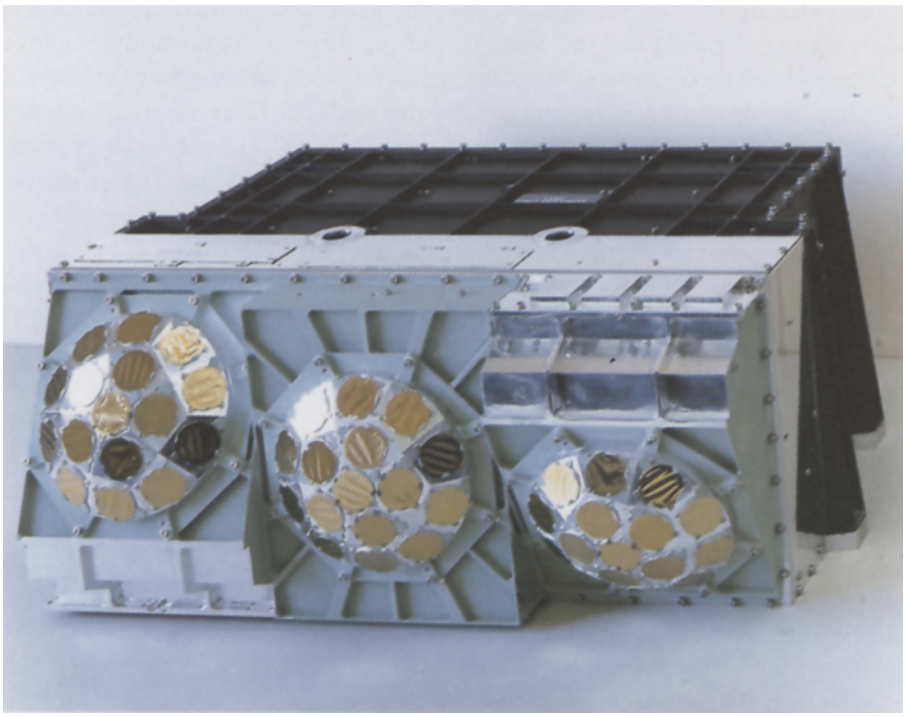

Fig. 3.2-1. Picture of the assembled LEMT system.

3.2. The Low Energy Matrix Telescope (LEMT) system

The completed LEMT system is shown in Figure 3.2-1.

LEMT Telescopes

A schematic cross-section and a front view of a LEMT telescope are shown in Figure 3.2-2. The front dE/dx elements are 16 surface barrier detectors arrayed on a spherical dome in order to minimize path-length variations. Each detector is nominally 1.75 cm^2 by 18 microns thick. The average thickness uniformity has been measured to be ± 0.34 microns (Barbier *et al.*, 1993). The residual E detector is an ion-implanted detector 36 cm^2 by 1000 microns thick. It is subdivided into five 13.3 mm wide strips on each side, strips on opposite sides being orthogonal

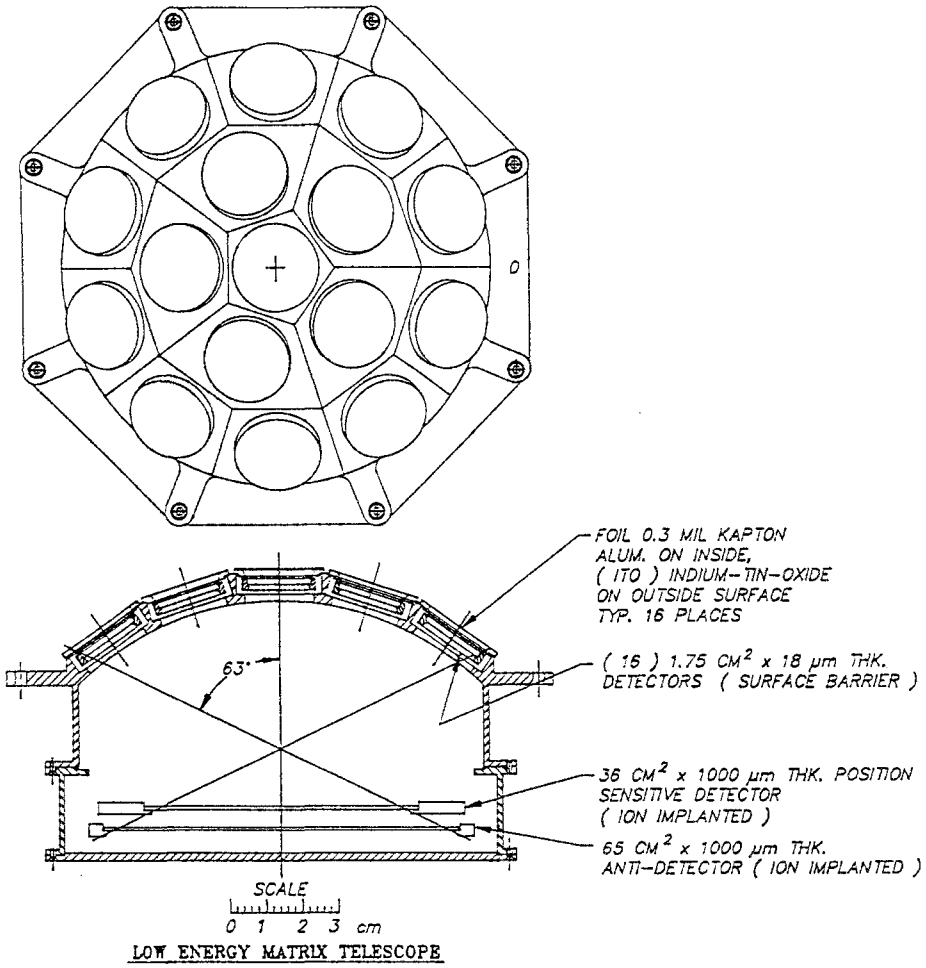

Fig. 3.2-2. Schematic cross-section and front view of a LEMT telescope.

to each other. Each strip has its own independent preamplifier. Cross-talk on the junction side is negligible, but on the ohmic side it varies from 1 to 10%. Behind the residual E detector is an anticoincidence detector to reject particles penetrating through the residual E detector.

LEMT Analog Electronics

The LEMT analog electronics is shown as a block diagram in Figure 3.2-3. The dome detectors (denoted by D) are connected to hybrid charge-sensitive amplifiers, which are followed by discrete bipolar shaping amplifiers. The shaped pulses are bipolar, have a peaking time of 3.4 μs, and return to baseline within 35 μs. The bias to each dome detector may be switched off individually in the event that a detector develops excessive leakage current or noise. The bias switches are controlled by

individual command bits which are set by ground command. Each strip of the position sensitive detector (PSD), or energy detector (denoted by E), has its own amplifier chain. The bias to the entire PSD may also be switched off by ground command.

Each shaping amplifier output is connected to a Lower Level Discriminator (LLD) and to an input of an analog multiplexer (MUX). Each LLD output can be enabled or disabled. Disabling is used during offset calibration of the PHA system to prevent contamination by particle signals, or in the event a detector/amplifier channel becomes excessively noisy or otherwise inoperative. The LLD outputs are connected to the same MUX. When a shaped pulse exceeds the discrimination level of the LLD, the LLD output triggers the MUX. The MUX logic then selects the analog input which corresponds to the LLD which triggered the MUX, and ignores all other inputs until a reset signal is generated by the CONTROL logic. The MUX also contains logic which encodes the input number of the active signal channel, and thus identifies the dome detector (or PSD strip) upon which the particle was incident. Knowledge of the detector location in the dome and $x - y$ location in the PSD is used to calculate azimuth and elevation of the incident particle. This information is subsequently used to apply a correction factor to the energy value to account for the trajectory-dependent path length in the dome detector. In addition, the dome MUX generates a 'multiple' signal if more than one LLD is active during the MUX cycle. This is necessary to reject the event, since more than one particle stopping in the PSD at one time would adversely affect the energy signal from the PSD. The dead-time for detecting successive particles in a telescope depends upon pulse height, ranging from 1.5 to 5.5 μs going from protons to Fe.

The 'multiple' rate is counted and when it becomes high enough, software can select higher LLD thresholds via command bits controlling the D and E reference generators. Higher thresholds reject the smaller, more numerous events, reducing system dead-time for the heavier elements.

The analog output from the MUX goes to a peak detector, a buffer followed by a high-resolution track-and-hold amplifier (T/H), and a 3-bit flash ADC. The presence and timing of the D and E peak pulses relative to each other are used by the control logic (along with other criteria) in determining whether or not to accept the event for pulse height analysis.

The 3-bit flash ADC performs coarse, but fast, pulse-height analysis at rates up to 180 kHz. The eight discrimination levels or 'bins' are approximately logarithmically spaced in the lower part of the dynamic range where H and He reside. The D and E axis discrimination levels are each encoded into three bits. These bits are presented to the address lines of a coincidence RAM together with four mode bits which select regions of the D versus E matrix for high resolution pulse height analysis. When rates are high, the mode bits can be set to select only heavier elements. Fast-analysis events can continue to be processed while a high-resolution analysis is being completed for a previous event. Thus the high-resolution portion

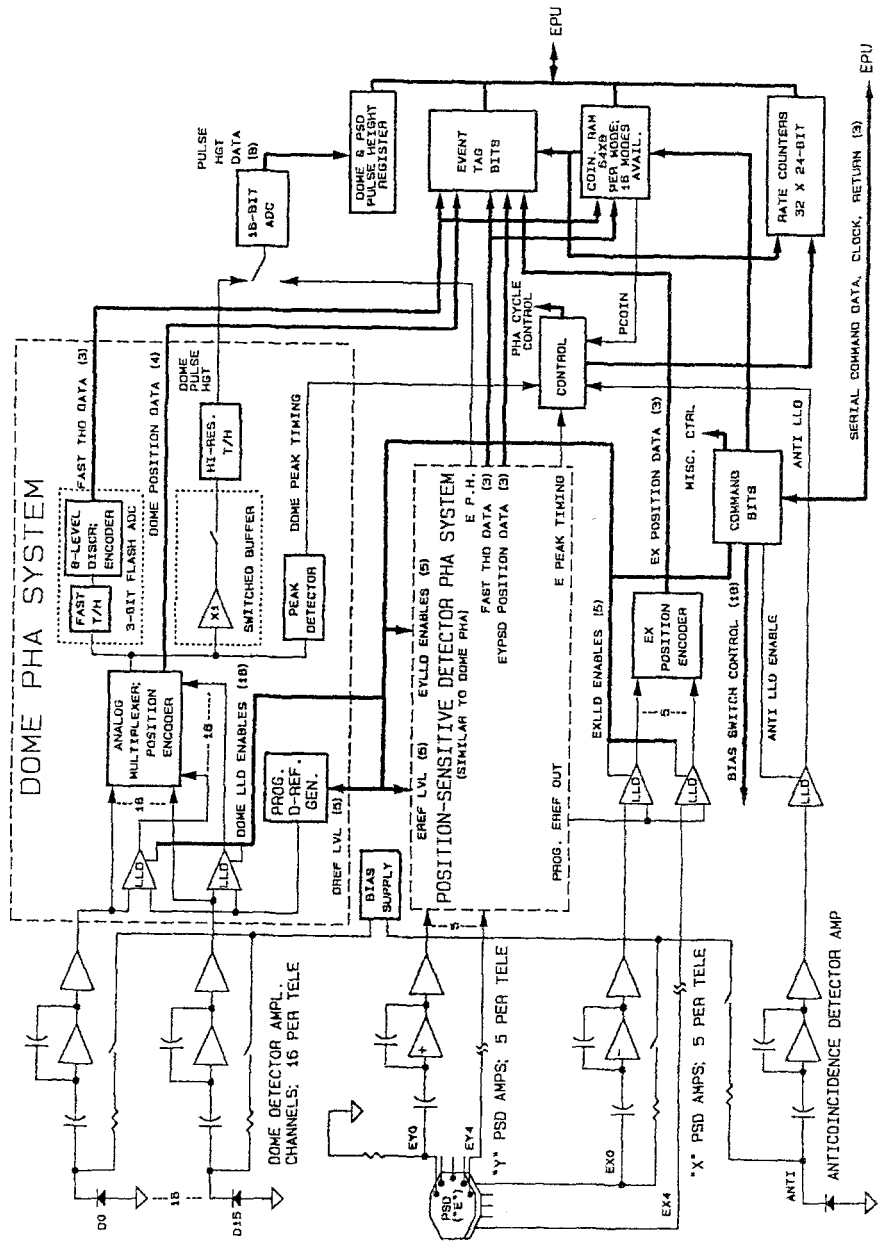

Fig. 3.2-3. Block diagram of the LEMT analog electronics.

of the PHA system is reserved for the rarer species, and is not clogged with more plentiful but less interesting events.

Hardware counters keep track of event rates in all the bins. An array of bins is organized into 16 'windows' in the 8 K $\times$ 8 coincidence RAM and the window rates are included in the telemetry. When the flash converter completes its cycle and the coincidence RAM generates the window number, a reset signal is sent to the MUX to put it in a state ready for another event.

When an event is accepted, the T/H goes into 'hold' mode when the shaped pulse reaches its peak value (as determined by the peak detector). This pulse height is then available for conversion to 16-bit binary data. The switched buffer prevents feed-through of any signals which may be present at the MUX output during the T/H hold period.

One 16-bit ADC is shared between the Dome and PSD systems. The T/Hs store the analog pulse heights and these outputs are switched to the ADC input at the appropriate times by the control circuitry. The ADC and associated control can handle complete events at approximately 23 kHz. Pulse height data from the ADC is stored in a register until it is read into the Event Processor Unit (EPU).

The PSD electronics are very similar to the dome system. The double-sided PSD has an 'energy' side (the top), in which both energy and strip number (y-coordinate) are read out. The PHA system contains the LLDs, MUX/encoder, peak detector, 3-bit flash ADC, T/H, and LLD reference generator as in the dome system. The 'multiples' output from the E-MUX is recorded with the pulse heights for each event but is not used to reject the event. The bottom side is used to read out an x-coordinate only, and hence only has LLDs and a strip number (x-coordinate) encoder. The x-LLDs use the same reference level as the y-LLDs. The PSD bias voltage can be switched on and off independent of any of the other bias voltages.

The anticoincidence channel contains only the amplifiers and fixed-reference LLD whose output is used to reject events. The anticoincidence detector bias voltage can also be switched on and off independently.

Registers store event bits for each high-resolution event. These event bits include the D and E fast ADC levels, the dome detector number, the x and y coordinates. an 'Ex-LLD Present' bit, and a fast-analysis window number.

Rate counters accumulate rates during each major telemetry frame. The quantities counted are D and E peaks, anti LLDs, coincidence information (peak timing okay, coincidence conditions passed, high-resolution PHA enabled), multiples, selectable dome LLD singles, and each window number.

The rates, tag bits, and high-resolution pulse height data are passed on to the EPU over a common data bus.

Sample Performance Data

Figure 3.2-4 shows some sample data taken at the Oak Ridge National Laboratory's Holifield Heavy Ion Research Facility. This figure combines data from multiple dome detectors for iron and silver beams incident on several different types of

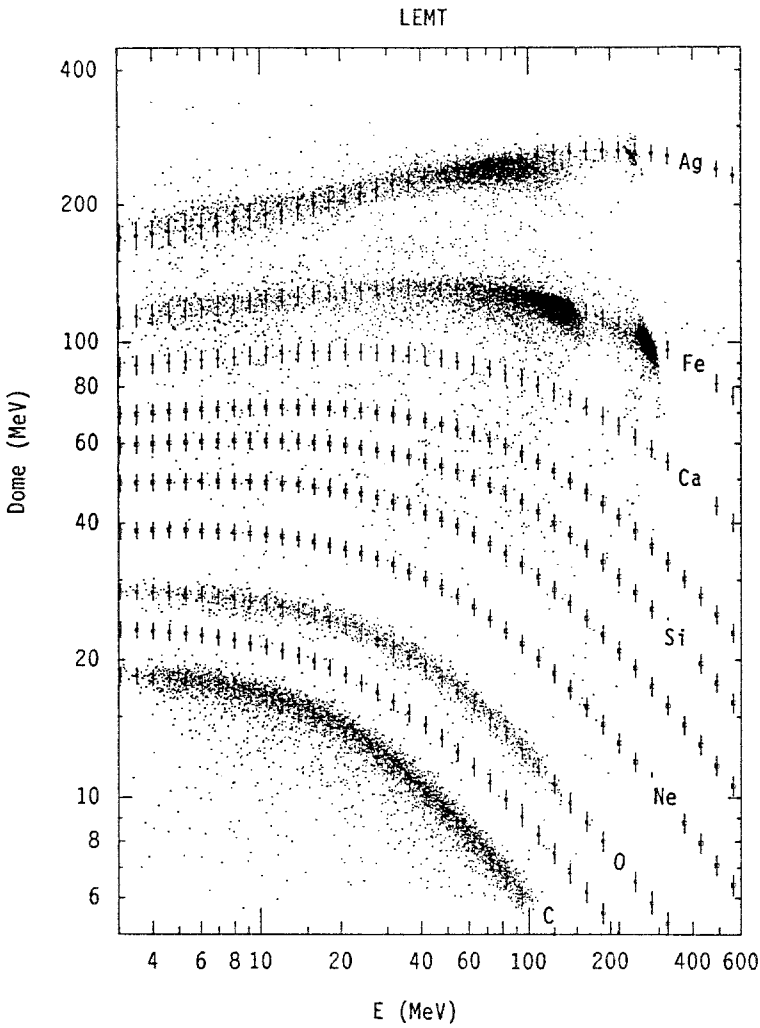

Fig. 3.2-4. Sample LEMT pulse height matrix. This matrix represents a sum of events from all three LEMT telescopes and for accelerated beams of Fe and Ag and coulomb-scattered C and O. Each D pulse height is corrected to a common detector thickness using the observed angle of incidence and the particular dome detector average thickness.

scattering foils. The C and O tracks were produced by coulomb scattering of the Ag beam from the plastic backing of a Ag scattering foil. Also shown are the expected track locations for various elements. The primary iron and silver beams were 450 and 550 MeV respectively. For the figure, the measured pulse heights have been corrected for their baseline offsets and converted to MeV. The dome detector pulse heights have also been corrected for the average thickness of the given dome detector and trajectory (this depends upon the specific dome detector thickness at normal incidence as well as the position and tilt of the dome detector relative to

the observed position in the position sensitive detector). These corrections make it possible to combine data for all dome detectors for all three telescopes into a single response matrix. These are the same corrections which are made by an on-board processing algorithm.

In terms of its particle resolution, the LEMT telescope was designed to be a multi-element version of the highly successful ISEE-3 VLET telescope (see e.g. Reames, Meyer and von Rosenvinge, 1994 and references therein). The pulse-height dynamic range was extended by a factor of $\sim$ 4 for LEMT to permit observation of ultra-heavy elements, whose abundances could be dramatically enhanced in small solar events. The actual resolution in charge (σ_z/Z) is $\sim$ 2% over the range from C to Fe, and is quite adequate to resolve the dominant element species shown in Figure 3.2-4. The largest contributor to the error in Z is thickness variations in the front detectors.

The accurate normalization of the response from different detectors depends upon a knowledge of the mean thickness of each dome detector. The mean response was measured by positioning each detector orthogonally to high energy beams at the National Superconducting Cyclotron Laboratory. The relative response of each detector to a 22.5 MeV amu^{-1} ^{16}O beam and a 39.5 MeV amu^{-1} ^{56}Fe beam were measured and found to be in agreement within 0.8%, on average. The mean detector thicknesses for the 48 dome detectors range from 14 to 18 microns. Dome detector response tables are loaded in the LEMT EPUs to correct individual particles as they arrive. In-flight corrections for particles traversing the telescope at arbitrary angles are made by separate look-up tables using the measured trajectory and the known instrument geometry.

3.3. The Electron Isotope Telescope (ELITE) System

The assembled ELITE system is shown in Figure 3.3-1. It consists of Alpha-Proton-Electron telescopes A and B and the Isotope Telescope.

The Alpha-Proton-Electron (APE) Telescopes

In principle the isotope telescope could observe minimum ionizing electrons and protons as well as stopping heavier nuclei. In practice, however, the dynamic range requirements in terms of energy losses and count rates are far too large. In addition, the energy loss dynamic range requirement is exacerbated by the fact that the energy-loss signal is subdivided in the IT Position Sensitive Detectors (PSDs) to obtain the particle trajectory. The primary purpose of the APE telescopes, then, is to provide coverage of the lowest charge particles over a wide range of incident energies up to very high rates. The APE telescopes do observe heavy nuclei up through iron, however, and can resolve isotopes of the lighter elements even without trajectory information.

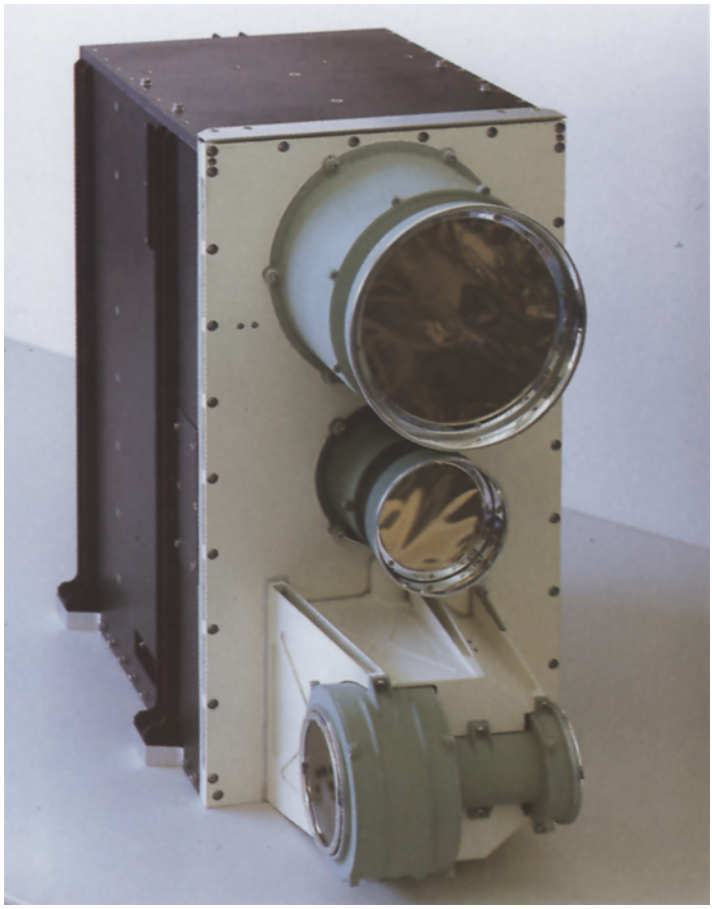

Fig. 3.3-1. Picture of the assembled ELITE system.

APE-A Telescope

Figure 3.3-2 shows a schematic cross-section of the APE-A telescope. The A1 and A2 detectors are circular silicon surface barrier detectors nominally 150 microns thick by 8 cm^2. The detector thickness was a compromise between wanting lower energy coverage of nuclei and being thick enough to observe electrons, which provide important time markers for solar events. Double foils are used in front of the telescope to protect the A1 detector from sunlight and from high counting rates due to particles at energies just below the APE-A energy range. Double foils provide better protection than a single foil against sunlight coming through pinholes in the vacuum-deposited aluminum applied to each foil. The A3 and A4 detectors are circular Lithium drifted detectors (LiDs) 3 millimeters thick by 17 cm^2. The telescope acceptance geometry is defined by a coincidence between the A1 and A2 detectors in anti-coincidence with the A4 detector. The geometry factor for the

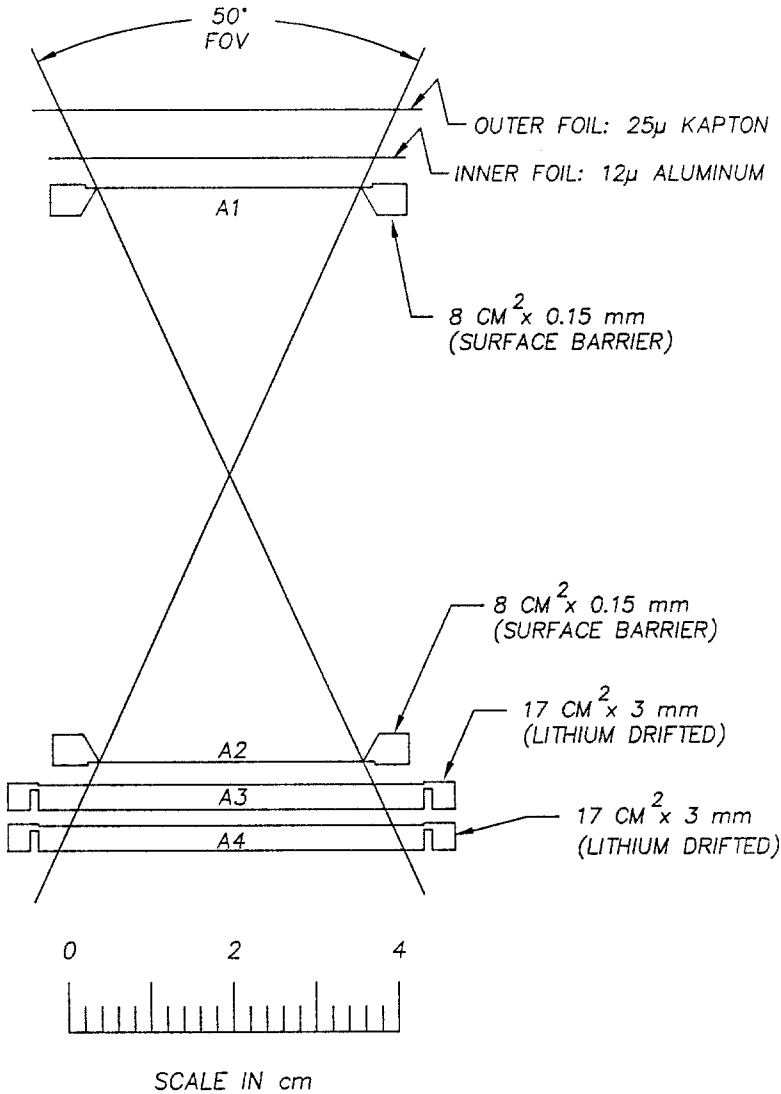

Fig. 3.3-2. Cross-section of the APE-A telescope.

APE-A telescope is 1.2 cm^2 sr, independent of energy. Other than the foils, there are no obstructions in the APE-A field of view.

APE-A Analog Electronics

Figure 3.3-3 shows a block diagram of the APE-A analog electronics. The signals from each detector are converted using double differentiation and double integration to bipolar pulses with a peaking time of 1 μs. Particles which pass through the A1 detector and stop in the A2 detector are referred to as 2-dimensional (2-D) events, while particles which pass through A1 and A2 and stop in A3 are referred to as 3-dimensional (3-D) events. Pulse height space is subdivided into rectangular areas and volumes using 4, 5, and 3 threshold discriminators on the A1, A2, and A3 pulse-height axes respectively. These are denoted $A1_0$, $A1_1$, ..., $A1_3$, $A2_0$, ..., $A2_4$, $A3_0$, ..., $A3_2$. These thresholds have been chosen such that electrons, 2-D and 3-D protons, 2-D and 3-D helium (alphas), and 2-D and 3-D heavy nuclei (charge $Z \geqq 2$) are completely contained in non-overlapping combinations of such rectangular regions. These combinations are encoded into the coincidence RAM. The size of the coincidence RAM has been kept small (2 kB) by encoding the discriminator outputs on each axis as the highest threshold level triggered. For example, the 5 threshold levels on the A2 axis can be reduced to 3 bits into the coincidence RAM. This is possible since triggering of one of the higher level thresholds implies triggering of all lower thresholds on the same axis. At the address lines of the coincidence RAM there are altogether 7 encoded threshold bits, 1 anticoincidence threshold bit, 1 hazard flag, and 2 latched command bits. The hazard flag indicates whether the current candidate event was preceded within the previous 10 μs by one or more pulses in any of A1, A2, or A3. The 2 mode bits are used to select events for pulse-height analysis. One is used to include or exclude hazarded events, while the other is used to include or exclude protons. The coincidence RAM is strobed by any $A1_0$ and $A2_0$ coincidence (denoted by $A1_0 \cdot A2_0$). Bit 0 out of the coincidence RAM is used to count all 2-D events, bit 1 is used to count all 3-D events and bit 2 is used to count penetrating events. Four additional bits out of the coincidence RAM are encoded to correspond to any one of the following mutually exclusive events: 2-D and 3-D electrons, 2-D and 3-D protons, 2-D and 3-D alphas, and 2-D and 3-D nuclei with charge >2. These same 4 bits together with 3 sector bits and the hazard bit make up a tag byte which is passed to the Event Processor Unit together with the A1, A2, and A3 pulse heights.

The A1, A2, and A3 pulse peaks are captured by sample and hold circuits and digitized by a single ADC in turn. All three pulse heights and the tag byte are put in a FIFO and transferred to the EPU (see Section 3.5), even for 2-D events. This leads to a fixed deadtime for pulse height analysis of $\sim$ 80 μs per event. New events which are detected by the coincidence RAM before the EPU has emptied the FIFO are processed and counted but are not accepted for pulse height analysis. Depending upon the relative pulse sizes, two events within as little as 2 to 10 μs of each other can be distinguished and counted. Every n Major Frames, where n can be set by ground command, the preamplifiers are turned off in order to eliminate particle pulses and the baselines are measured and transmitted to the EPU.

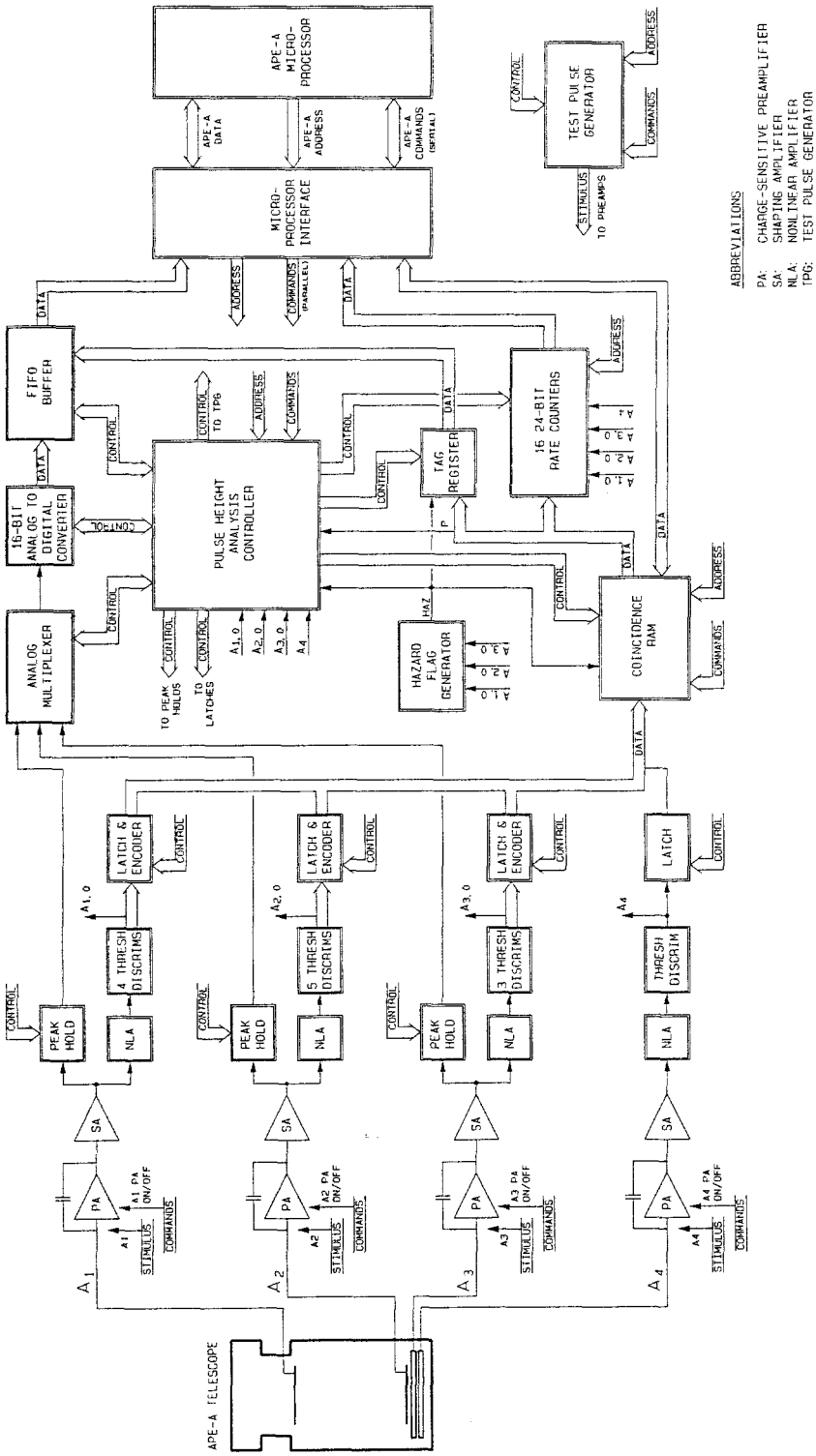

Fig. 3.3-3. Block diagram of the APE-A analog electronics.

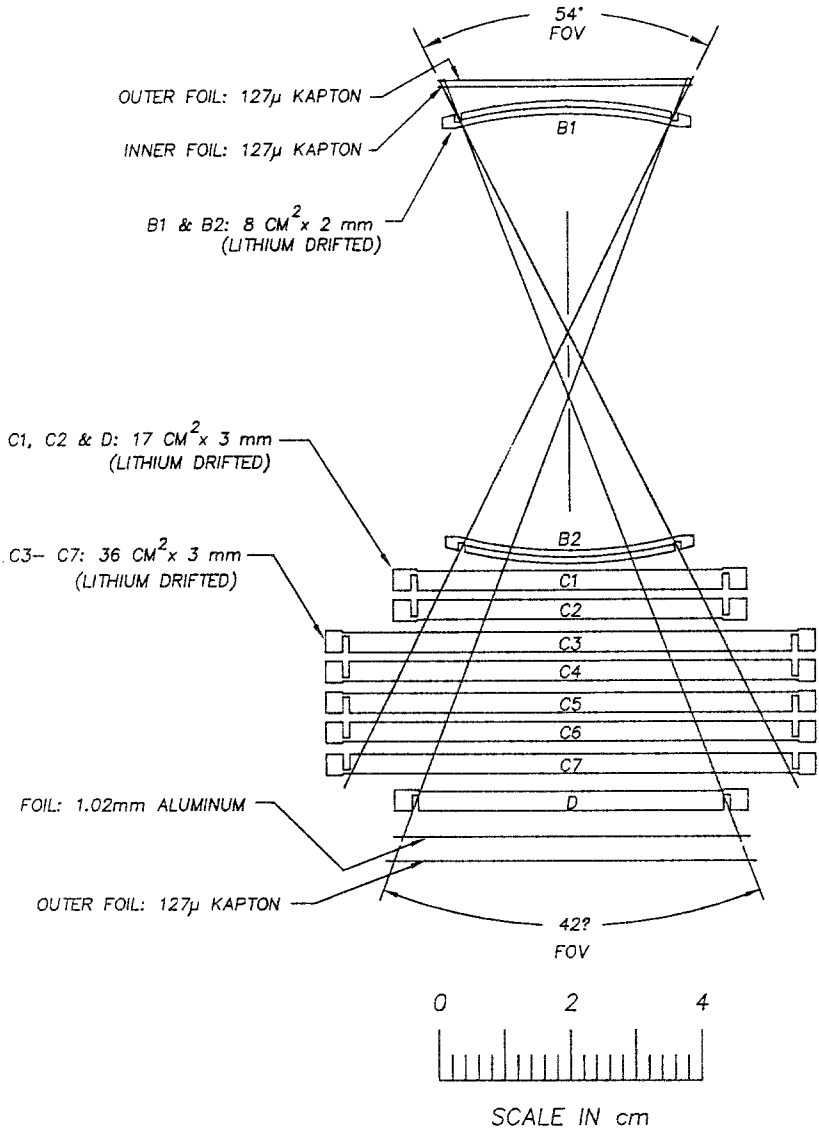

Fig. 3.3-4. Cross-section of the APE-B telescope.

Each of the preamplifiers has protection so that high voltage breakdown of any of the detectors will not destroy the input FETs.

APE-B Telescope

Figure 3.3-4 shows a cross-section of the APE-B telescope, which consists entirely of Lithium drifted (LiD) detectors. The B1 and B2 detectors are curved (mean

radius of curvature = 7.0 cm) to minimize pathlength variations (Perkins *et al.*, 1969). The maximum variation is 2.8% for particles not passing through an edge of B1 or B2. Particles stopping in APE-B are identified by the coincidence condition $B1_0 \cdot B2_0 \cdot \sim C7$ (where $\sim$ means not). The geometry factor for stopping particles is 1.3 cm^2 sr, independent of energy. Particles stopping in B2 are referred to as 2-D particles, while those penetrating B2 and stopping in one of C1 through C6 are referred to as 3-D particles. Approximately 12% of stopping particles pass through an edge of B1 and/or B2; many of these can be rejected for 3-D events by requiring that the B1 and B2 pulse heights be consistent. Penetrating particles, i.e., particles satisfying the coincidence requirement $B1_0 \cdot B2_0 \cdot D$, are also accepted for analysis. This expands the energy range to include minimum ionizing particles. Penetrating particles include both particles which enter through the B1 detector and exit through the D detector (forwards particles) and those which enter D and exit B1 (backwards particles). Forewards and backwards particles can be distinguished only for the lowest energy penetrating particles. Hence a measurement of penetrating particles, to be uncontaminated by high energy particles interacting in the obstructing material, requires unobstructed view angles 180° apart. APE-B has been mounted on a short tower protruding from the spacecraft in an effort to meet this requirement. The forwards view angle (for stopping particles) is obstructed only by the double foils indicated in Figure 3.3-4. The backwards view angle, however, is obstructed slightly (5%) by the spacecraft. The magnetometer boom covers an additional 15% but presents an amount of mass/unit area which is small compared to the thickness of the telescope. The geometry factor for the penetrating particles, allowing for the 5% loss due to the spacecraft, is 1.95×1.08 cm^2 sr.

LiD detectors have a deadlayer on the grooved (signal) side. This is a thin layer which is overdoped with Li and which, to zeroth order, appears to be inactive. The thickness of this layer is usually measured using a collimated electron source (e.g., Bi^{207}, 0.972 MeV electrons, range in Si = 1.7 mm) exposed alternately to the two sides of the detector. The difference in energy loss observed between the two sides divided by dE/dx for the electrons ($\sim$ 0.36 keV μm^{-1}) is the nominal thickness of the deadlayer. The deadlayer is, of course, not really sharp and some charge will diffuse out of the deadlayer and be collected. The amount of charge collected will depend in part on the length of the charge collection time. We found that the initially-measured dead layers were substantially less than were subsequently observed during accelerator calibrations with heavy nuclei. We attribute this to the relatively short time constant (0.79 μs) used for both APE-A and APE-B in the flight electronics as compared to that initially used to measure the deadlayer. There is also a loss of pulse-height amplitude (the so-called 'ballistic deficit') associated with the finite time for charge collection of charge created in the depletion region of the detector. This is largest for the holes which have a charge collection time up to 0.4 μs in C1 through C6. For double differentiation/double integration with time constant τ the ballistic deficit is given by

$$\text{B.D.} = -0.065\left(\frac{T}{\tau}\right)^2,$$

where T is the charge collection time. For the holes, then, this amounts to 1.5%.

APE-B Analog Electronics

The performance of the analog electronics for APE-B (Figure 3.3-5) is very similar to that for APE-A but with the inclusion of penetrating events. The pulse height channels are B1, B2, the sum of outputs from the C1 through C6 detectors, denoted C_{1-6}, and D. All four pulse heights and the tag byte are put in a FIFO and transferred to the EPU (see Section 3.5), even for 2-D events. This leads to a fixed deadtime of $\sim 100\ \mu$s per pulse-height analyzed event; the resolving time for counting individual particles is ~ 2–$10\ \mu$s, depending upon pulse-height. Baselines are measured in concert with APE-A and transmitted to the EPU.

Sample Performance Data

Figure 3.3-6 shows a histogram for data taken with the APE-B telescope at the Bevalac at the Lawrence Berkeley Laboratory. The quantity Z' is calculated using the formula presented in section 4.1. The accelerated beam was 258 MeV nucl^{-1} Fe incident on a polyethylene target well upstream from APE-B. The emerging beam consisted of Fe fragments, primarily due to interactions with protons in the polyethylene. Individual elements are clearly resolved up to at least Ca. Similar performance has been obtained from APE-A using lower energy beams at the National Superconducting Cyclotron Laboratory at Michigan State University.

APE-A and APE-B performance has also been measured using ^{4}He beams of varying energy and intensity. Penetrating sea-level muons are routinely observed in APE-B. Unfortunately, to date there have been no measurements with protons or electrons for APE-A or APE-B. The expected energy ranges of coverage for protons and electrons in each APE telescope are presented in Table I.

The Isotope Telescope (IT)

The IT Telescope

Figure 3.3-7 shows a schematic cross-section of the IT telescope. The first two detectors are two-dimensional position sensitive detectors (PSDs). They are required so that path-length corrections may be made for the angle of incidence and for non-uniformities in detector thickness. Tungsten rings are used to mask off circular areas for each PSD as illustrated in Figure 3.3-7. The electrodes on each side of each PSD are segmented into 125 strips with a pitch of 0.5 mm and an inter-strip gap of 35 μm. As shown in Figure 3.3-8, the strips are interconnected by chip resistors (68 ohms each) at the periphery of the detector wafer. Preamplifiers connected to strips 1, 32, 63, 94, and 125 subdivide each PSD surface into 4 sections of 32 strips each. When a particle passes through a strip between two preamplifiers, the charge is subdivided between the preamplifiers in amounts which depend upon the number of discrete resistors between the signal strip and each of the two

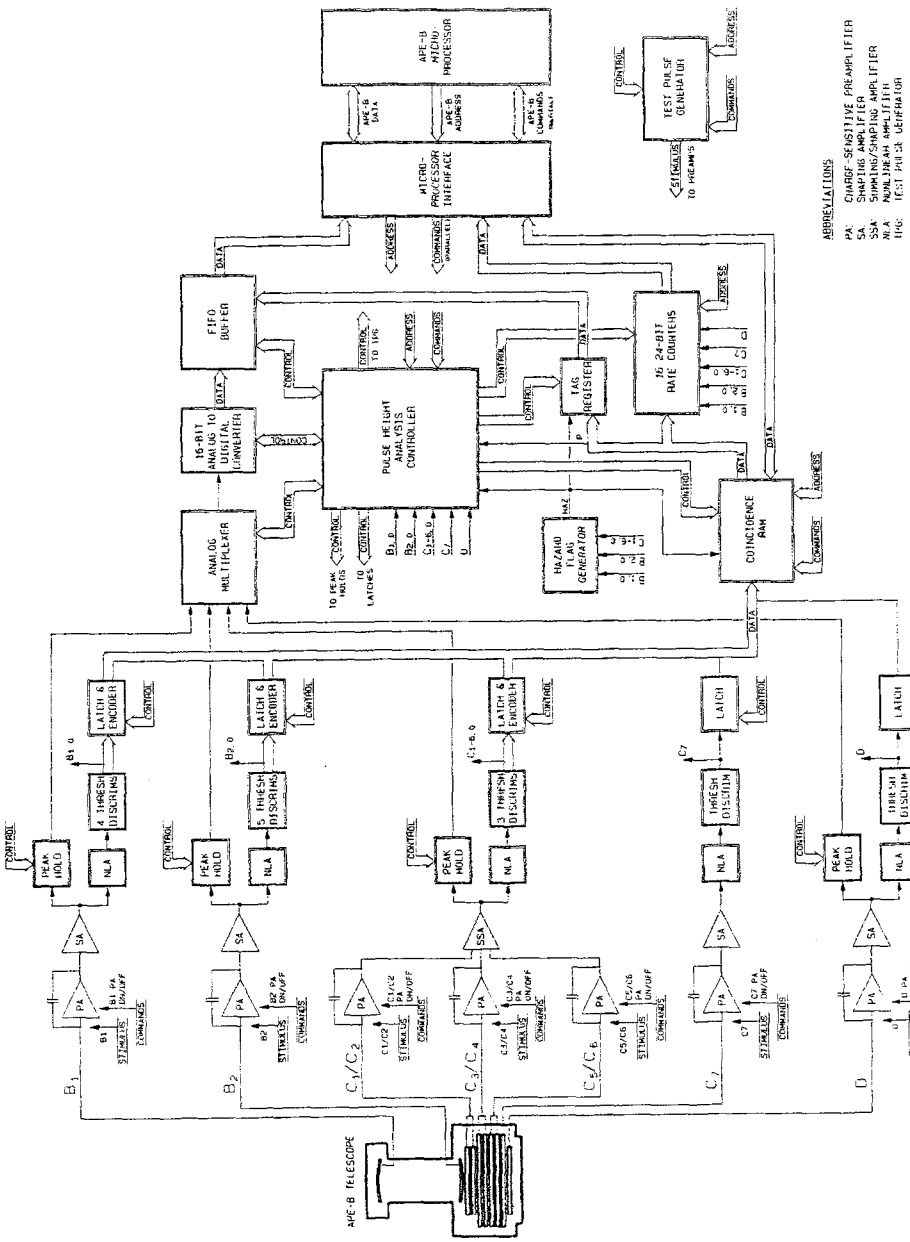

Fig. 3.3-5. Block diagram of the APE-B analog electronics.

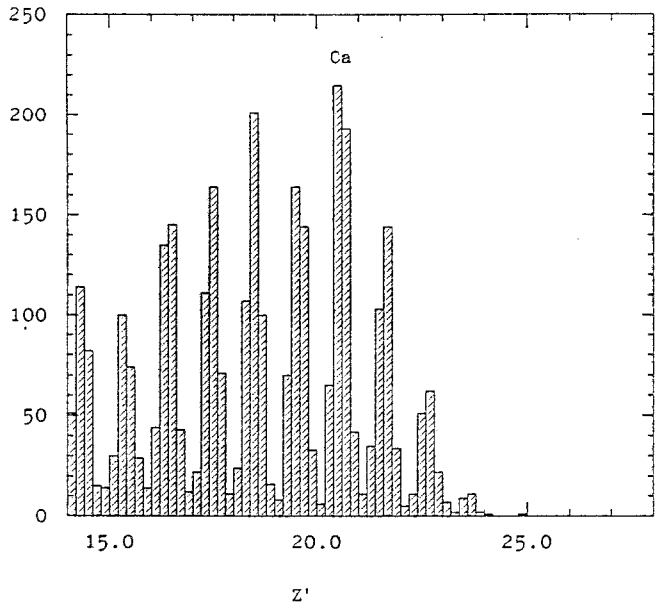

Fig. 3.3-6. Sample histogram of APE-B data. The x-axis is Z', an estimate of the incident particle charge, which is defined in Section 4.1.

preamplifiers. Thus the two pulse heights give a measure of the particle position. This is illustrated in Figure 3.3-9, which is a scatter plot of pulse heights in two adjacent preamplifiers. Note that each strip corresponds to a locus of events. For the small signals associated with He nuclei, it is not possible to resolve individual strips, but it is also not necessary since the isotopes of He are easily separated with even poor spatial resolution. The reasons for subdividing the detector surface into 4 separate sections are that (1) subdivision by 32 rather than 125 reduces the dynamic range requirement by a factor of 4, (2) the detector capacitance for one section is approximately one fourth that for the whole detector, reducing both the ballistic deficit and cross-talk between preamplifiers on opposite sides of the detector.

The E1, E2, and E3 detectors are surface barrier detectors. This avoids problems with dead layers. LiD detectors are used for the rest of the stack (E4, E5a, and E5b and the anticoincidence detector E6) because E3 is about as thick a detector as can be made with surface barrier (or ion-implant) technology. Detector thickness increases systematically with depth in the stack in order to minimize Landau fluctuations. Ballistic deficits associated with charge collection are only a consideration for the PSDs (see below); in principal these are systematic, knowable effects which can be corrected. The strip loci in Figure 3.3-9 appear to lie on an essentially straight line without sag in the middle, suggesting that ballistic deficit is not a serious problem for the PSDs either.

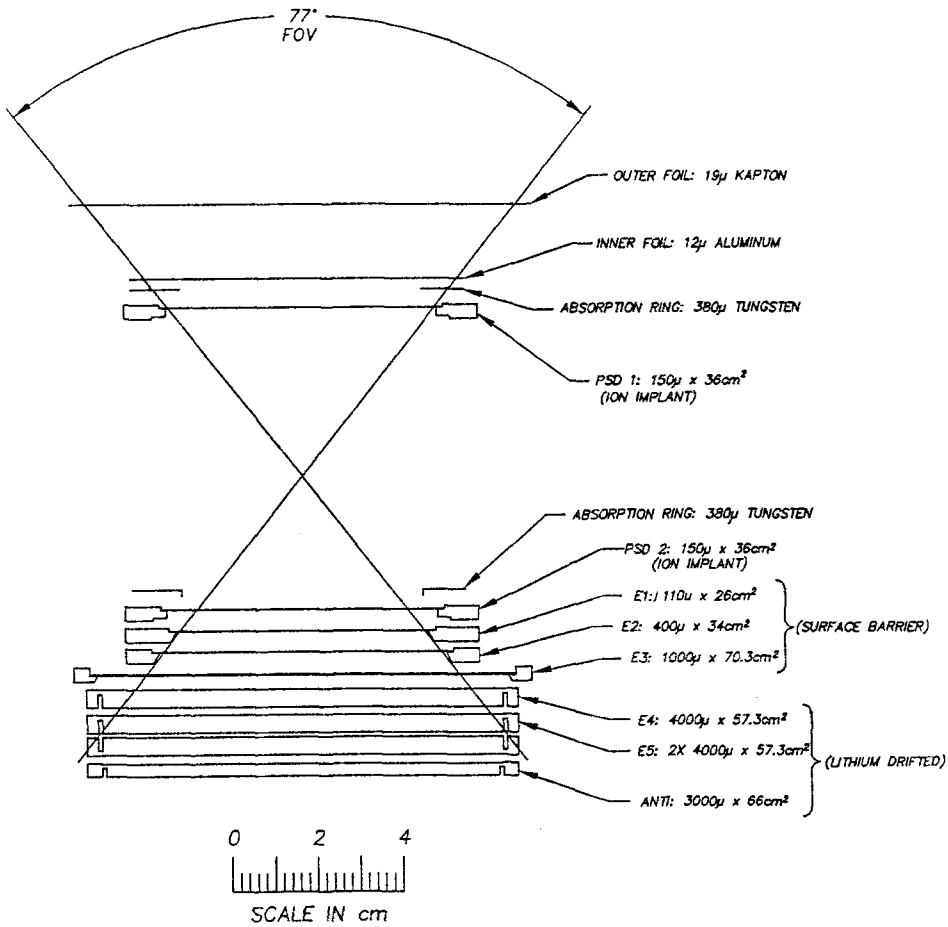

Fig. 3.3-7. Cross-section of the Isotope Telescope.

IT Analog Electronics

Figure 3.3-10 shows a block diagram of the IT analog electronics which processes the signals received from the stack of 2 position sensitive detectors, 5 energy detectors (E1 to E5) and one anticoincidence detector (E6). These signals are amplified, pulse shaped, pulse height analyzed as 25 PHA channels, and passed on to the onboard microprocessor module, the EPU. A brief description of the various subsystems and their functioning follows:

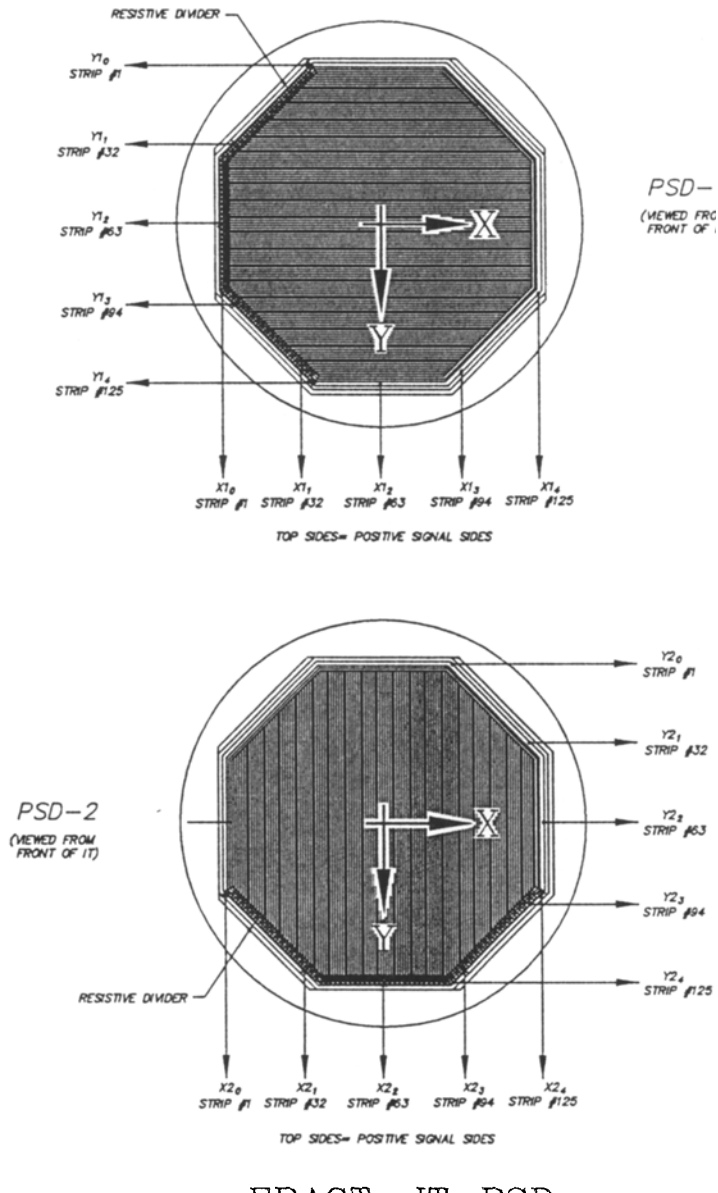

Fig. 3.3-8. Top views of the two 2-dimensional position sensitive detectors, PSDl and PSD2, for the Isotope Telescope.

Preamplifiers: a total of 26 preamplifiers are connected to the stack ofdetectors as follows: 10 for each of the two PSDs (PSD1 and PSD2) and 1 for each of E1 to E6. All the preamplifiers are configured as charge amplifiers and also provide high

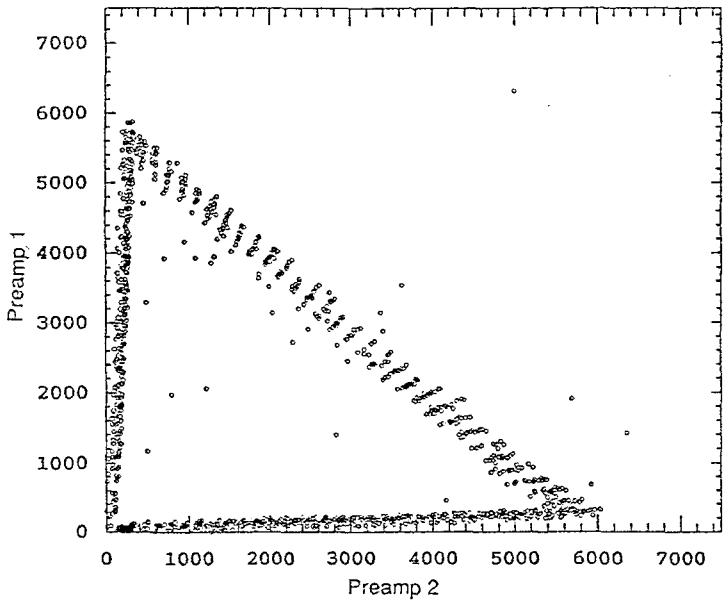

Fig. 3.3-9. Pulse height matrix for two adjacent preamplifiers on a 2-dimensional position sensitive detector in the Isotope Telescope. Note the clustering of points, one cluster per strip in one of the four sections of the PSD. The data points along the x- and y-axes correspond to particles passing through the two adjacent sections of the detector.

voltage bias to their respective detectors. Each of the preamplifiers has 3 inputs, one from the detector, one for an external pulser, and a third input from one of the 3 onboard test pulse generators.

All preamplifiers are DC-coupled to post or shaping amplifiers which are described below.

Shaping amplifiers: there are 26 unipolar shaping amplifiers connected to an equal number of preamplifiers. All the shaping amplifiers can be characterized as having one zero and three poles. The zero in each of the shaping amplifiers is adjusted to cancel the corresponding pole of its preamplifier.

The peaking times of the various shaping amplifiers are as follows: 1.8 μs for each of the 20 PSD channels and 4.5 μs for each of the 6 E channels.

For single differentiation/double integration with time constant τ as used here, the ballistic deficit is given by

$$\text{B.D.} = -0.021 \left(\frac{T}{\tau}\right)^2 ,$$

where T is the charge collection time and τ is half the peaking time. Holes in the 4 mm thick LiD detectors (500 V bias) have a charge collection time = 0.67 μs and hence a ballistic deficit of 0.2%. The PSDs have charge collection times which are due to the resistive divider and the detector capacitance. Ballistic deficits in the PSDs are potentially more serious: if we take the total resistance and capacitance

for the largest section, then the RC time constant is 1.5 μs and the corresponding ballistic deficit is 5.8% (worst case). As mentioned earlier, the ballistic deficit for each strip is, in principal at least, knowable and can be corrected.

Peak holds: there are 25 peak hold circuits which hold the peak values of the unipolar pulses obtained at the outputs of the shaping amplifiers. The outputs of the peak holds are made available to the ADCs for pulse height analysis. Each peak hold has an FET switch at its input which is switched to an open or high impedance state a short time after the peaks have been captured and is switched back to the closed state after all the channels have been digitized and the digital data passed on to the EPU.

Discriminators: there are 19 discriminators also connected to the outputs of the shaping amplifiers as follows: 2 for each of the E1 through E5 channels, 3 for E6, and 3 for each of PSD1 and PSD2. All the discriminators have a Robinson type base line restoration at their inputs. The input signal for each PSD discriminator is obtained from a nonlinear summing amplifier that sums up the 5 shaping amplifier signals originating from the positive electrode side of the PSD.

For each detector, one threshold is set to an energy approximately 20% higher than a proton can deposit in the detector. These are OR'd together in the Rates Logic block of Figure 3.3-10 to form OR1. Similarly there is one threshold for each detector which is approximately 20% higher than a ^{4}He can deposit. These are OR'd together to form OR2. Computer simulations show that OR1 cleanly separates proton events from heavier events, while OR2 separates He from heavier events (very occasional Li nuclei may fail to trigger OR2). Protons are not analyzed at all by IT. A commandable mode bit includes/excludes He from analysis.

There are 3 different discriminators for the anticoincidence detector. Initially we anticipated that E4, E5A, and E5B would each be segmented into a central detector area and a surrounding guard ring. It was planned to sum the guard ring signals together with the signal from E6 to form an overall anti-coincidence signal. Cross-talk between the central areas and the guard rings for large signals in the central areas could then potentially trigger the anticoincidence even though the particle did not actually enter E6 or one of the guard rings. The three different discriminator levels were intended to differentiate between cross-talk and particles actually entering the anti-coincidence 'detector'. The anticoincidence level for analysis can be commanded to any one of the three levels (or none); each pulse height event tag word contains the states of these three discriminators. Obtaining the Si for the LiD detectors proved to be very difficult and cutting the extra grooves for the guard rings could have reduced the yield. Ultimately it was decided to only use E6 as the anticoincidence detector. Inspection of Figure 3.3-7 shows that some particles can exit out the sides of E5A and E5B; the on-board algorithm has to reject trajectories for which this is possible since there are no guard rings.

Peak detectors: there is a peak detector associated with each of the two PSDs. The inputs are obtained from the nonlinear summing amplifiers. Coincidence of

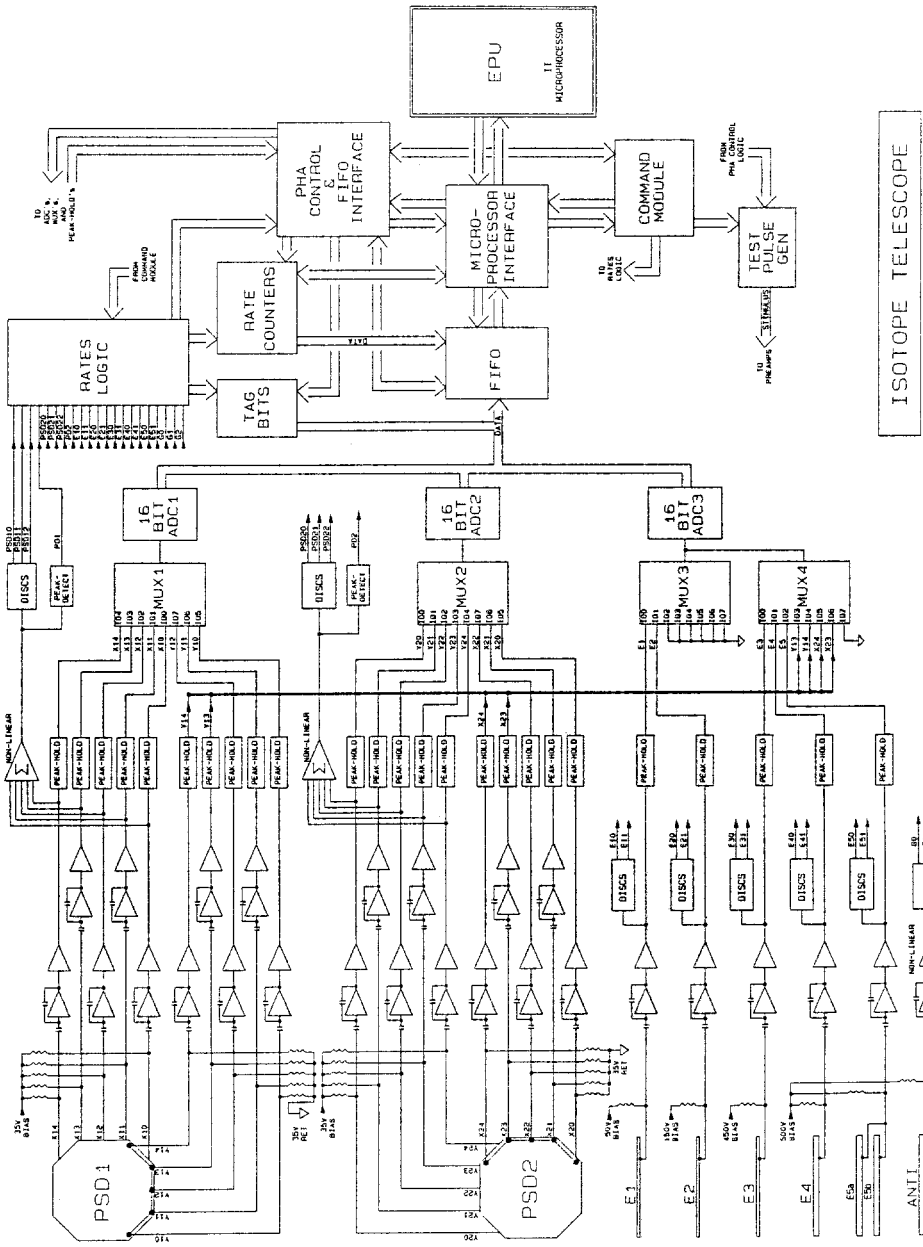

Fig. 3.3-10. Block diagram of the analog electronics for the Isotope Telescope.

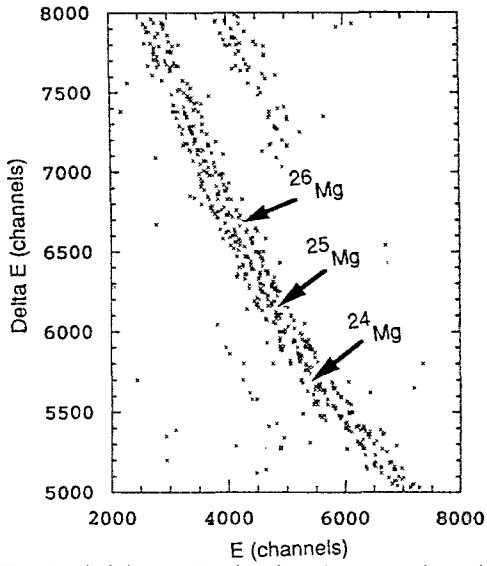

Fig. 3.3-11. Sample IT pulse height matrix showing the separation of the isotopes of Mg. No thickness map corrections have been made to this data.

the two outputs is used by the logic circuit to trigger a possible analysis of the event.

ADC and data capture circuits: there are a total of 3, 16 bit, successive approximation type ADCs used to pulse height analyze 25 channels. Each ADC has an analog multiplexer (MUX) at its input; two of the MUXes have 8 inputs and the third has 9 inputs. The outputs of all the ADCs are tristate and are tied together to form a local data bus that is connected to the FIFO input. The ADCs have an approximate conversion time of 25 μs. Control logic steps the 3 MUXes in parallel, initiates pulse height analysis in each of the 3 ADCs and then transfers the results to the FIFO. At the end of the 9th conversion cycle a data available signal is generated for the EPU to receive the data. The time measured from the occurrence of the event to the data available going high is approximately 218 μs and a typical time measurement for the EPU to read the FIFO is 76 μs, thus giving a total busy time of 294 μs. However, the busy time can be longer than 294 μs if the EPU is busy when data available goes high and therefore delays reading of the FIFO.

To prevent damage to the ADCs due to high power dissipation during an unintentional latchup state, the current to the ADCs is continuously monitored and the power supply to the ADCs is automatically shut off under such a condition.

Rate counters: there are 32 24-bit counters which are read by the EPU every spin. IT rates are not sectored.

PHA control/Logic unit: this unit generates all the timing signals and conditions required to operate the peak holds, MUxes, ADCs, and the FIFO. It also interfaces with the onboard microprocessor unit, the EPU. This unit incorporates the serial

transmit/receive chip (referred to as the Command Module in Figure 3.3-10) which communicates serially with the EPU. The command bits controlling the operation of the IT are received and held by this chip.

Sample Performance Data
Figure 3.3-11 shows a scatter plot of data taken at the National Superconducting Cyclotron Laboratory at Michigan State University. The isotopes of Mg are clearly separated in this figure. No detector thickness map corrections have been applied to this data. These corrections will need to be applied in order to have adequate resolution for the relative abundances expected for energetic particles in space. This will be the subject of a future paper.

3.4. THE *SUPRATHERMAL ENERGETIC PARTICLE* (STEP) SYSTEM

Figure 3.4-1 shows a photograph of the assembled STEP system. The protective doors, shown in the open position in the photograph, provide an extension of the sun-shades at the entrance to each STEP telescope. Additional shading from solar radiation is provided by the flaps on the sides of each door, visible in Figure 3.4-1.

STEP Telescopes
Figure 3.4-2 shows a schematic cross-section of a STEP telescope. The front foils are each 1000 Å of nickel mounted on a mesh. Acoustic vibration tests to simulate the launch environment lead to openings in a small number of cells of the mesh. The microchannel plates and foils were replaced prior to launch. Operation of these telescopes is described in the next section.

STEP Electronics
A block diagram of the STEP electronics is shown in Figure 3.4-3.

The measurement technique used in STEP is Time-of-flight vs Total E. In each of two identical telescopes, incoming nuclei enter through a pair of thin (1000 Å) nickel foils, pass through a time-of-flight region and strike a surface barrier silicon solid state detector located at the rear of the telescope. The detector is thick enough to stop all particles of interest and the detector signal thus represents the total energy of the particle. This energy signal is detected by a standard charge-sensitive amplifier, shaped by a shaping amplifier with peaking time of approximately 1 μs and run through a set of discriminator amplifiers and a pair of parallel linear amplifiers of differing gain. Two amplitude discriminators set to $\sim$ 80 keV and $\sim$ 10 MeV allow us to determine that a particle has struck the detector and to select which of the two linear amplifier outputs to analyze. The high gain linear amplifier generates a full scale output for an input of about 12 MeV, the low gain channel handles up to about 60 MeV. Having two 'ramps' in this way provides a wide dynamic range without sacrificing resolution at the low end.

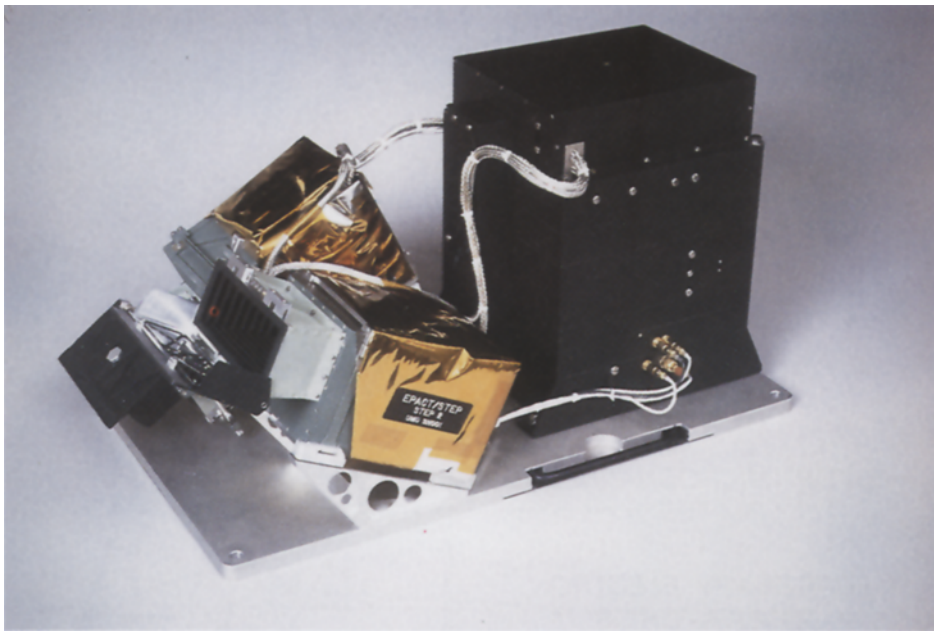

Fig. 3.4-1. Photograph of the assembled STEP system.

In parallel with the energy, the time of flight is analyzed. As the incoming ion passes through the inner nickel foil, it knocks a few ($\sim$ 4–30) secondary electrons off the inner surface of the foil into the TOF region. These electrons are accelerated by a 1 kV potential within the chamber and are directed toward a chevron pair of microchannel plates (MCPs) which detects them and multiplies them by roughly 107, producing a measurable signal. The MCP assembly is called a SEDA (secondary electron detection assembly) and the output signal is designated START. A similar STOP signal is derived from the back-scattered secondary electrons produced when the incoming ion strikes the front surface of the solid state detector. The time between the two signals equals the time taken by the ion to traverse the TOF chamber and is typically 2–100 ns. The START and STOP signals are processed through constant-fraction discriminators to reduce 'walk' and drive a time-to-amplitude converter (TAC) whose output amplitude represents the time-of-flight of the ion. Logic circuitry is used to detect the coincidence of a STOP signal occurring within 100 ns of a START and signals this coincidence by generating a 'Valid Stop' pulse. Note that there is a single TOF electronics system servicing both telescopes. While not ideal, this design saves a considerable amount of mass and, particularly, power over a two-TOF system and works because the dead time for a TOF signal (a few hundred ns) is small compared to the expected count rate (a few thousand per second).

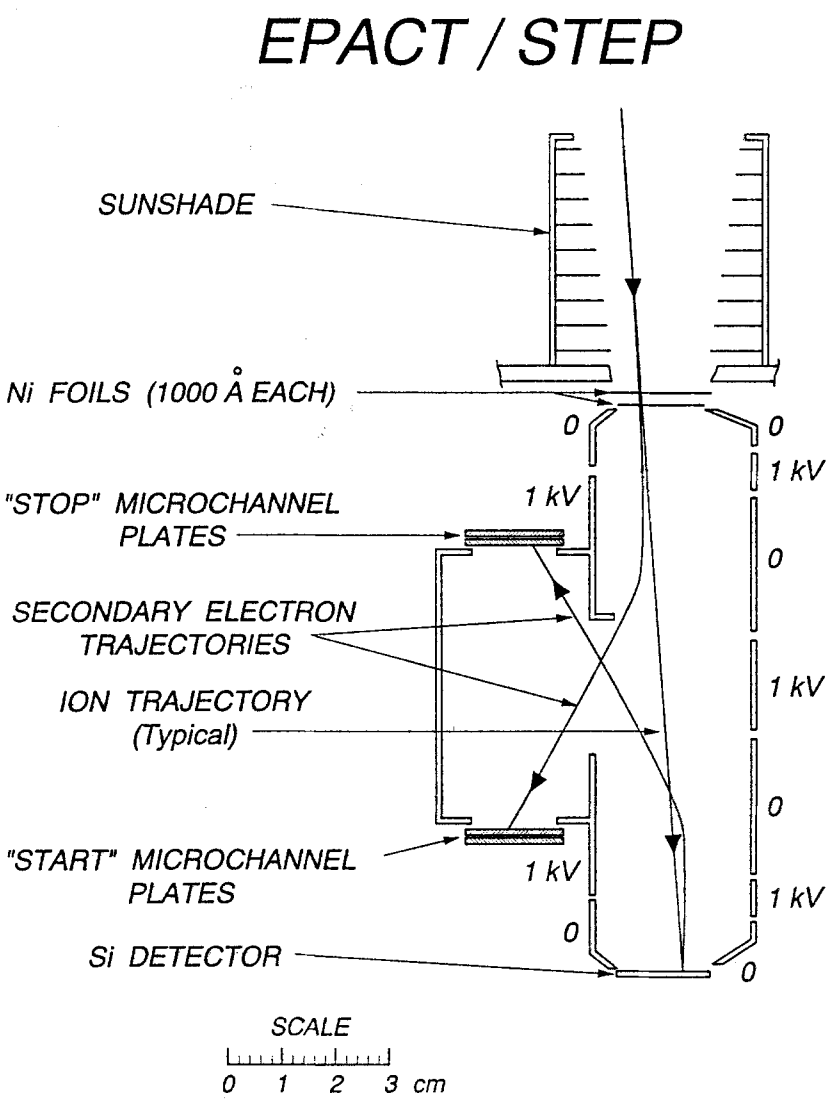

Fig. 3.4-2. Cross-section of a STEP telescope.

The TAC and energy linear amplifier signals are fed to a 'Slant' amplifier which forms a weighted analog sum and determines whether or not the particle has mass >4. This is used to assign *a priority* on further processing of the event, heavies receiving higher priority. In fact, since constant mass lines form curves in TOF-E space, a single weighted sum is insufficient to determine mass and the circuit

actually performs a 4-piece linear approximation to the actual curve, forming 4 sums and ANDing the four discriminator outputs to generate the final result.

A Valid Stop which occurs at the same time as a solid state detector discriminator pulse indicates that a particle of interest, or 'event', has been detected by the telescope and this coincidence causes 'event processing' to begin. The output of one of the energy linear amplifiers (determined by which discriminators fired) and the TAC output are pulse-height analyzed (Height to Time Converters: E – 10 bits + ramp indicator, TOF – 9 bits) and stored with other identifying information in an event buffer. A low-power 1802 microprocessor collects the event, sorts it according to the approximate logarithm of the TOF and energy into one of 86 bins representing different mass and energy ranges (Matrix Rates) and sends it to the data processing unit in ELITE. The System Processor Unit sums each Matrix Rate into 8 accumulators, one for each $\frac{1}{8}$th of a spin, over an integral number of spins for each Major Frame.

In addition to the event-based data, discriminator 'Serial' rates (Singles, Valid Stop, TOF-E Coincidence) are accumulated in hardware counters (GSFC 633, PMOS rate accumulator chips) and are read out to the DPU once per sector. Analog housekeeping data (temperatures, HV monitor) are multiplexed out to a single 0–5 V analog housekeeping line. Digital housekeeping is generated in the 1802 and sent periodically to the DPU. The 1802 processor operates at approximately 0.1 MIPS and uses 2k bytes of RAM and 4k bytes of ROM (1kB program, 3kB table lookup). Apart from the processor and the rate accumulator chips, the remaining logic is all CD4000-series CMOS.

Other blocks in Figure 3.4-3 include:

– In-flight stimulus – generates paired analog energy and TOF signals and sends them to the front-end electronics, simulating incoming particles and exercising the entire analog and digital electronics chain.

– LVPS – a standard crystal-controlled DC-DC converter operating from 28 V and providing the low voltages required by the remaining STEP circuitry including bias voltage for the solid state detectors and primary power to the HVPS.

– HVPS – a low-power converter that generates the voltages between 950 V and 3.5 kV needed to accelerate and detect the secondary electrons in the TOF telescopes. The lower voltages are all derived as fractions of the highest output, which is selectable by ground command.

– Heaters – of two types. The actuator heaters are used once after launch to warm the paraffin motors which unlatch and open the acoustic covers over the two telescopes. Once open, these covers remain so throughout the mission. The other heaters are survival heaters (described earlier).

Sample Performance Data

Figure 3.4-4 shows sample performance data taken at the Brookhaven National Laboratory Tandem Van de Graaff. The figure is a scatter plot showing time of flight versus residual energy measurements for incoming beams of helium,

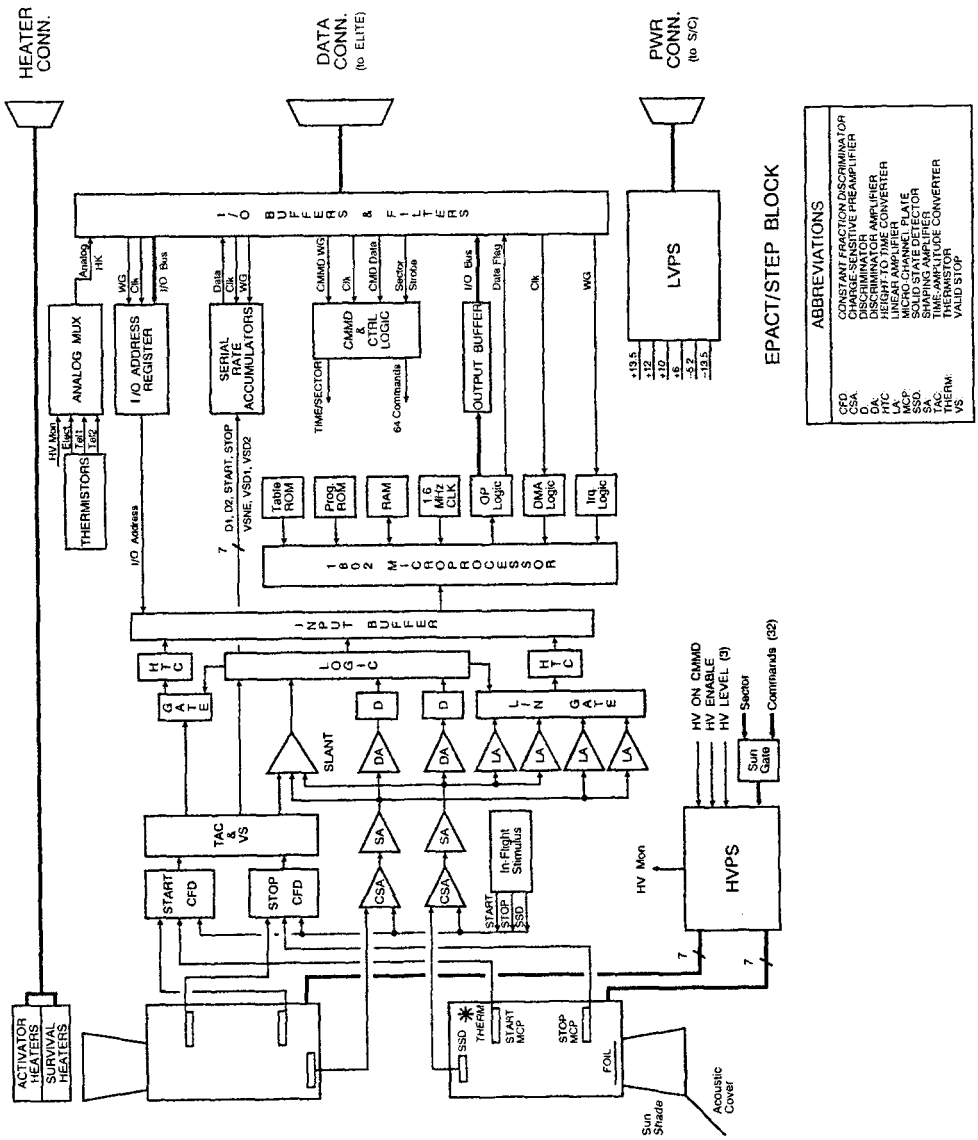

Fig. 3.4-3. Block diagram of the STEP electronics.

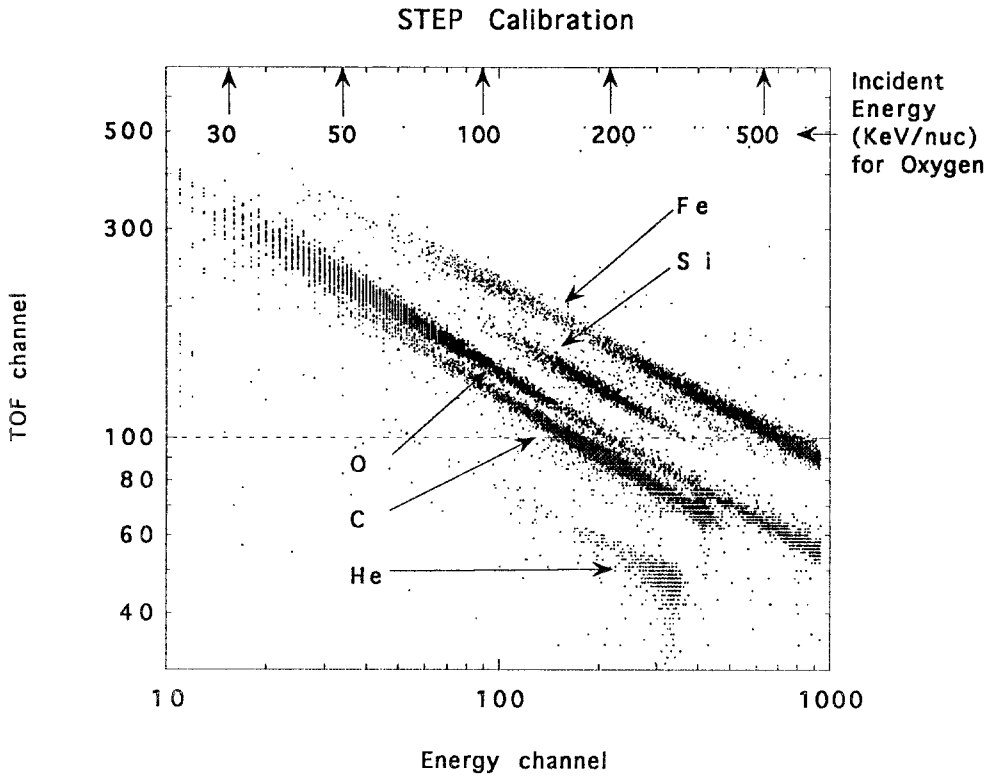

Fig. 3.4-4. Example of heavy ion tracks from STEP calibration runs for beams of He, C, O, Si, and Fe. The accelerator beams passed through foils before entering the STEP telescope, broadening the range of energies. The scale at the top indicates the incident energy for oxygen nuclei.

carbon, oxygen, silicon, and iron. Each dot on the plot represents one analyzed ion. Although monoenergetic beams were used in this calibration, they passed through foils in front of the telescope, with the result that a large range of incident energy particles entered the telescope, populating long sections of the tracks as shown. The correspondence between location in the scatter plot and particle incident energy is indicated on the top of the figure for oxygen. It can be seen that the STEP instrument resolves major ions down to energies below 100 keV nucl^{-1}.

3.5. THE LEMT/ELITE DATA PROCESSOR UNIT

The EPACT common Data Processor Unit (DPU) is shown in Figure 3.5-1. The hardware design is identical for both instruments, LEMT and ELITE, except that the STEP interface card is only present in the ELITE DPU. The basic design consists of a two level computing architecture that meets the requirement for similar spacecraft interfaces and functions, yet supports entirely different onboard data reduction algorithms for a diverse set of telescopes. At one level, the System Processor Unit (SPU) interfaces to the WIND spacecraft, providing command,

telemetry, and housekeeping functions. The SPU also services the next level of computing which consists of three Event Processor Units (EPU). Each EPU is a dedicated compute engine, interfacing to front-end pulse height analyzer (PHA) electronics and performing event processing algorithms for a particular telescope. Unlike the EPU, the STEP interface card is not microprocessor based; it serves only to emulate the avionics interface for which STEP was originally built.

Event Processor Unit (EPU)

The EPU design is based on the UTMC UT1750 16-bit microprocessor (UTMC, 1990a) operating at 10 MHz. In this application it is used in its native RISC mode to achieve better performance (at least four times) than in the MIL-STD-1750A emulation mode. It is a dual-bus Harvard architecture device which has separate instruction and operand busses. Each bus has a 16K byte RAM memory bank using IBM 6408 memory chips. There is no non-volatile memory on the EPU. All EPU program code is downloaded from the SPU at boot time. Both EPU memory banks are dual port accessible between the 1750 and the 80C86. The SPU can either halt an EPU and access its memory, or simply perform interleaved cycle-stealing accesses. The EPU ingests raw pulse height processed events and hardware accumulated rates. The event data is processed according to a telescope specific algorithm with the results placed in operand memory. Later, the SPU retrieves data from all EPUs prior to telemetry formatting.

As part of the digital design effort, two semi-custom gate arrays were developed on UTMC's rad-hard process (UTMC, 1990b). One of the devices, the SXR (for Serial Transmitter Receiver) is a multi-personality chip that can be used at either end of a serial, synchronous communications data link. It is used in the SDX (Serial Data Transmitter) master configuration in the EPU to command and verify discrete control bits in the front-end electronics of a telescope. There it is used in the SDR (Serial Data Receiver) slave configuration to receive intra-instrument serial commands, decode them, latch command control bits, and return the status of these bits when requested. The third 'personality' of this device is a 'glue' logic chip in the LEMT analog electronics. The other gate array developed, named 'EC1624', implements sixteen 24-bit counters with flexible counting and readout options. A total of ten of these chips were used in EPACT, substantially reducing the resource needs for hardware event counters. Both gate array designs are detailed in Winkert (1992).

System Processor Unit (SPU)

The SPU design is based on the Harris 80C86RH 16-bit microprocessor operating at 4MHz. The adjoining 82C85RH clock generator chip contains a crystal controlled oscillator and provides clock conditioning for reset and wait state timing. The chip's 'divide-by-256' feature is utilized when the SPU is commanded into a power reducing 'slow' mode. This reduces the processor clock to 15.6KHz during software idle periods, realizing a 58% power saving for the SPU board ($\sim$ 14%

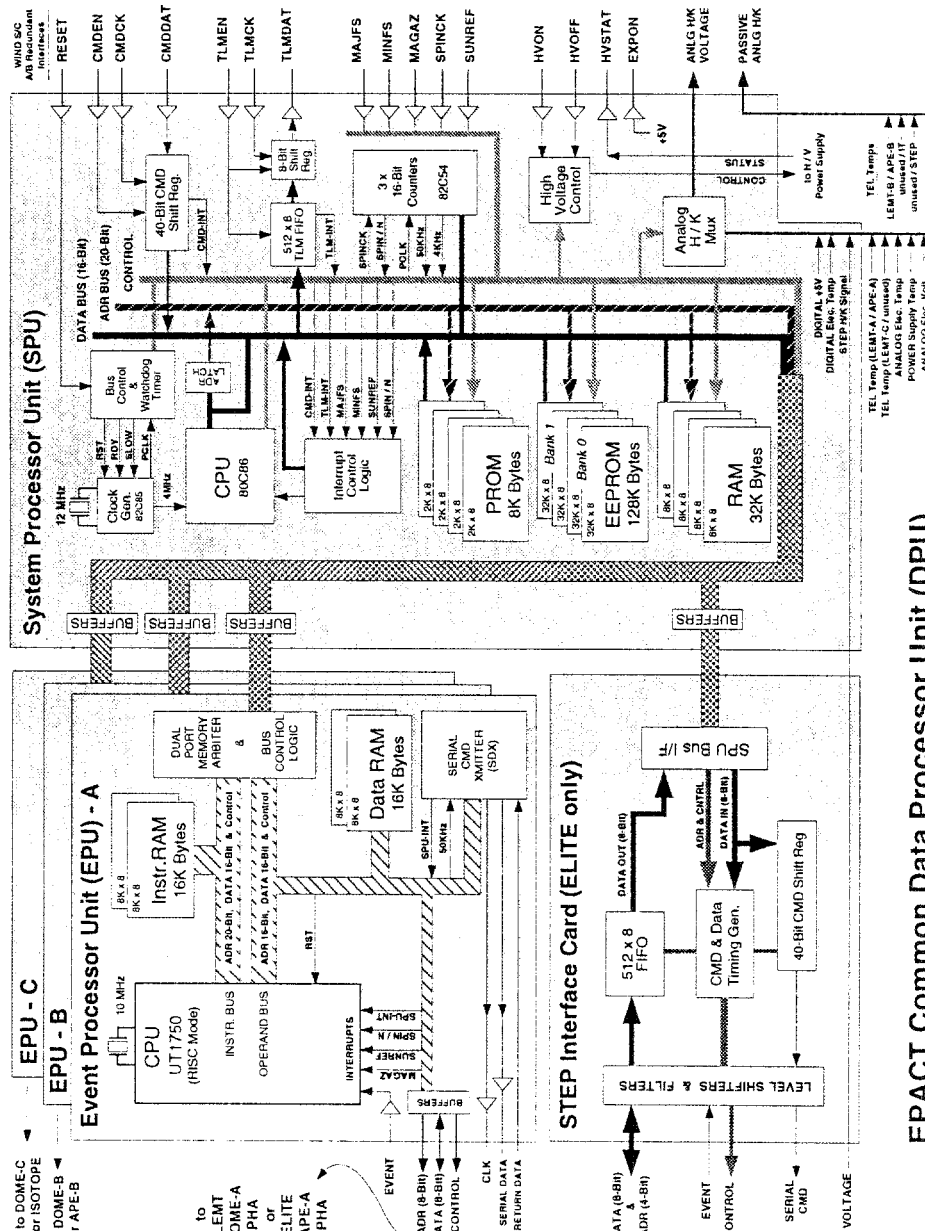

Fig. 3.5-1. Block diagram of the EPACT Common Data Processor Unit. Separate copies are used by the LEMT and ELITE systems. Each Event Processor Unit processes the events from a single particle telescope. The STEP interface card is used by ELITE only.

for the whole DPU). SPU flight software is interrupt driven by six conditions: command received, telemetry FIFO full, major frame sync, minor frame sync, Sun reference pulse, and spin sector boundary. Interrupt priority is automatically resolved by the 80C86 via its vector driven table lookup. A watchdog timer must be cleared by software at least once every four minor frames (92 ms at the fastest telemetry rate) or else a processor reset is generated.

The SPU onboard memory consists of three types of storage: permanent read-only memory (8K bytes of CMOS fuse-link PROM), non-volatile electronically erasable programmable memory (128 K bytes of CMOS EEPROM), and volatile random access memory (32K bytes of CMOS static RAM). In addition, each EPU memory block is memory mapped into a separate 64 K-byte segment of the 80C86 one megabyte address space. Boot code and parameter driven core software functions are stored in radiation hardened PROM (Harris 6617RH devices). The EEPROM memory (SEEQ 28C256 devices), is organized as two 64 K byte banks for redundant sets of parameter tables and EPU downloadable code. These parts were screened to 30 Krad total dose plus tested for latchup and single event upset (SEU) levels. They were found to be susceptible during write cycles but this is not of great concern because they are only write accessed during very infrequent memory uploads. Each entity stored in EEPROM also has an internal sumcheck so that data integrity can be monitored. The RAM memory is implemented with rad-hard IBM 6408 devices.

4. On-Board Software

4.1. Event Processor Unit (EPU) software

With the exception of STEP, each EPACT telescope has a supporting *E*vent *P*rocessor *U*nit (EPU) containing a 1750 microprocessor running in RISC mode. STEP contains an 1802 processor and has its own interface to the 8086 SPU where some EPU-like functions are performed.

In general, each EPU receives pulse height events which are queued for processing and also put into readout queues. Hardware rates are counted in the EPU rate counter chips, and are read out into EPU RAM and cleared on spin or spin sector boundaries. Software rates are bins into which PHA events are counted after undergoing analysis in the EPU software to identify particle species and energy interval. SPU software has tables which can be modified, but its software is hard-coded into PROMs. By contrast, the EPU software is fully replaceable by upload via serial commands from the ground.

LEMT

Event Processing

The three telescope domes on LEMT are controlled by identical copies of the event data analysis software on each EPU, but with different tables specifying the physical

characteristics and geometry of the individual domes. Event analysis begins when the PHA signals the EPU through an interrupt. Within the interrupt service routine, the raw pulse heights and flag bits are read in, then the event is placed in one of three queues for protons, He nuclei, or heavy ions based upon its 'window' number from the coincidence RAM. The queueing system ensures that any heavy ions that arrive are captured and processed with the highest priority, followed by He nuclei, then protons with lowest priority. In the main processing loop, the input queues are checked according to a priority round-robin scheme. The pulse height offsets are subtracted, logarithms of the corrected pulse heights are obtained, and then corrected by the detector geometry. The corrected D and E pulse heights are fed into a lookup table to obtain the software bin into which the event falls, and the software counter is incremented. The lookup table also specifies whether the particular software rate is sectored, in which case the software counter is found by adding the telescope azimuthal look-angle to the current spin or magnetic azimuth sector count. The software can identify and count more than 10 000 events per second. The geometry and detector thickness maps, the matrix lookup tables, and the sectoring information are all contained in uploadable tables within EEPROM. Instrument reconfiguration is accomplished by uploading new tables, which require a hard reset to take effect.

Rate Processing

Hardware rate counters are read and cleared by the EPUs on spin boundaries, except for the D-Singles and PHA rates which are accumulated according to spin sector. The two sectored hardware rates are fixed, and not configurable by table uploads. Hardware rates are summed into software counters in EPU RAM, then read and cleared on Major Frame spin-aligned boundaries by the SPU. Non-sectored rates are individually log-compressed from 24 to 16 bits for telemetry. Sectored rates are block-compressed from 24 to 8 bits, with a common exponent transmitted in an additional 8 bits.

Mode Control

Coincidence mode criteria are controlled by the SPU software. After each Major Frame is read out, the SPU examines the hardware rates and selects one of 16 coincidence maps in the coincidence RAM for use during the next Major Frame accumulation. In this way the software adapts to high particle fluxes by throttling down the number of low priority particles that will be admitted for software analysis. The coincidence tables are also uploadable, providing another layer of operator control.

Baseline Calibration

Under SPU control, the pulse height baseline offsets for the D and E pulse height analyzers on each dome are measured at commandable intervals. The EPUs remain active, and the baseline measurements are captured by the EPU as if they were

normal pulse heights. The offsets are averaged into the previous readings and stored in EPU RAM. The baseline calibration takes most of a spin to complete, so one spin is dropped from Major Frames in which the calibration is performed.

APE-A

Event Processing

Events in APE-A are flagged in hardware according to whether they stopped in A2 or A3. When a PHA event is ready the interrupt service routine reads the PHA data and flags, latches the spin sector count, and places the event in a queue for processing. The queue is only two events deep, and two events of the same type are not allowed. This gives equal time to protons and heavier elements. In the background processing loop, events are extracted from the queue, baseline offset corrected, and identified by an algorithm described in detail elsewhere (von Rosenvinge *et al.*, 1993). Briefly, given a particle of total energy E passing through a detector of thickness Δx and emerging with energy E', the following equation gives a measure of the particle charge (and mass):

$$Z' = \left(\frac{K}{\Delta x\, 2^{\gamma-1}}\right)^{1/(\gamma+1)} (E^{\gamma} - E'^{\gamma})^{1/(\gamma+1)} ,$$

where K and γ are characteristic of energy loss in silicon. The algorithm obtains bin indices for Z' and for the kinetic energy/nucleon and uses these to look up a corresponding software counter number. In the case of 3-D events, two estimates of charge are obtained, one using A1 as Δx and one using A2 as Δx. These two estimates are required to be consistent (i.e. have the same bin indices). The algorithm has been optimized for speed as well as accuracy. For example, the gain of A3 is exactly set to one eighth the gains for Al and A2. This permits left shifting the A3 pulse height 3 times and adding to the Al and A2 pulse heights in order to obtain E, thus avoiding an integer multiply. The algorithm can identify and count more than 7000 events per second.

When an event has been identified, the corresponding software counter is incremented. Some telemetry space is allocated to full event readout together with the computed software counter number. Processed events are placed into one of four output queues to optimize event coverage.

Rate Counters

Hardware rate counters are read out and cleared by the EPU on a spin basis or a sectored basis. Thirteen hardware rates are summed in EPU RAM for a whole spin-aligned Major Frame. The SPU reads out and clears the summed rates each Major Frame together with the number of spins. Three other hardware rates may each be spin sectored either relative to the magnetic field direction or relative to the direction of the Sun according to commandable parameters. There are also 47 software rates. Four different sectored software rates are arbitrary combinations of any of the 47 software rates. These combinations are contained in a commandable

table. All APE non-sectored rates are logarithmically compressed from 32 bits to 16 bits for telemetry readout. APE sectored rates are block-compressed from 24 bits to 8 bits with a common 8-bit exponent.

Baseline Calibration
Baseline calibration is performed under SPU control at commandable intervals (nominally every 16 Major Frames). The EPU is halted, then the detector baselines are sampled eight times and averaged. If the variance is less than a threshold value, the new baselines are placed in EPU RAM; otherwise they are discarded. The baseline calibration takes most of a spin to complete.

Mode Control
APE-A has four separate modes which are controlled by two mode bits. One of these controls whether hazarded events are pulse-height analyzed and the other controls whether protons are pulse-height analyzed. These bits are set by ground command.

APE-B
The APE-B data processing is essentially the same as APE-A event processing with the addition of penetrating events. Penetrating events are not analyzed in software, but are placed in a separate output queue. The APE-A and APE-B pulse height events share a single telemetry packet. If there are many events available from each, then the packet is shared equally. If, on the other hand, there are no APE-A events but many APE-B events, the packet will be filled with APE-B events. This is eased by the fact that, while there are 4 non-zero pulse heights passed to the EPU for penetrating events, only three pulse heights are transmitted to the ground: (B1+B2)/2, C_{1-6}, and D. Thus all APE pulse height events are the same length.

IT
Event Processing
Each IT event consists of 25 16-bit pulse heights and a tag word. The pulse heights are converted to floating point energies and the remaining computations are all done in floating point format. The event analysis results in computed values for Z', Z'', and E, which are converted into integer form for readout. Here Z' and Z'' are two estimates of the particle's mass computed from an equation similar to that used for the APE telescopes:

$$Z' = \left(\frac{K}{\Delta x_0\, 2^{\gamma-1}}\right)^{1/(\gamma+1)} (\cos\theta(E^{\gamma} - E'^{\gamma}))^{1/(\gamma+1)} .$$

Here the particle pathlength in the $\mathrm{d}E/\mathrm{d}x$ detector is given by the normal incidence thickness, Δx_0, divided by the cosine of the angle of incidence, θ. The $\cos\theta$ is determined from the PSDs. The particle trajectory is projected to the $\mathrm{d}E/\mathrm{d}x$ detector in order to obtain a thickness correction factor which takes into account

the thickness non-uniformity of the detector. These on-board thickness maps are contained in 32×32 arrays. Great care must be taken to ensure that the thickness maps correspond to the actual physical orientation of each detector in the stack. This is the first attempt to identify isotopes on-board. The on-board algorithm is capable of processing approximately 200 events per second.

IT has a number of readout modes with varying degrees of compression. In the fully expanded mode, all 26 event words, Z', Z'', and E are telemetered. In the intermediate mode, the PSD strip numbers, the last four energy losses in the telescope, E, a depth byte, and a compressed tag word are telemetered, requiring 8 words per event. The depth byte gives a measure of the vertical depth the particle has reached in the last detector entered. In the fully compressed mode, only Z', Z'', E, the depth byte and the compressed tag byte are returned. In the fully expanded mode and the nominal 92 s per Major Frame, it takes 4 s to read out a single event; the fully compressed mode reads out events $\sim$ 7 times faster. To compensate for these slow readout rates, the heaviest nuclei are given the highest priority for readout.

Rate Counters

The 32 hardware rate counters and 13 software rate counters are read out and cleared on spin boundaries by the EPU, and accumulated in EPU RAM. The summed values are read out and cleared by the SPU each spin-aligned Major Frame. The hardware rate counters are log-compressed (24 bits to 16), but the software counters are not.

Baseline Calibration

Baseline calibrations are performed automatically at commandable intervals. The EPU remains active, and the baseline event is read by the EPU. Normally the event is identified by its flag bit, and placed in a buffer for the SPU. The SPU averages the baselines into the existing average, and the new baselines appear as the first IT event in the next Major Frame. A diagnostic mode exists in which the calibration events are simply passed into the telemetry output buffer in the EPU without SPU intervention.

Mode Control

IT can be commanded into several different states, all by ground command. Helium can be included or excluded from being analyzed. The anticoincidence threshold for E6 can be set to any one of three different levels: the anticoincidence function can also be turned off altogether. The readout format of pulse height events can be set to expanded, intermediate or compressed, allowing 23, 83, or 166 events to be read out Per Major Frame.

STEP

Because STEP was added to EPACT after the initial design of each, STEP does not have an EPU per se. The functions of its 1802 microprocessor were described

briefly above. The remaining on-board processing for STEP is performed by the ELITE System Processor Unit.

STEP requires that a specific sequence of commands, synchronized to the spin pulse train, be sent to it in order for it to keep track of the spin sector, and to read out the information it accumulates. This is accomplished in the flight software using two separate functions, both in the SPU, one operating synchronously and one operating asynchronously.

The synchronous function gets called 64 times per spin. This function is in charge of issuing all of the commands to STEP. The spin count is divided down so that things basically happen 4 times per spin sector. The reason for this timing is to keep a steady flow of information coming back from STEP without crowding the FIFO. On two of the four sector subdivisions, the spin sector count is sent to STEP, resulting in 16 spin sectors. STEP latches this count at the next spin pulse, which allows it to measure sector boundaries precisely.

The asynchronous function gets called from the 8086 background loop. It checks the STEP FIFO to see if a transmission from STEP to ELITE, initiated by the synchronous function, is complete. If the FIFO contains STEP data, it is read out and placed or accumulated in the appropriate software counters. For sectored rates, the sector that was in effect when the command was sent is used. When the entire Major Frame has been read out, all of the software counters are copied, with compression where required, into the STEP output frame buffer. For matrix rates, the software counter in which to accumulate each rate read out is found in a lookup table, indexed by the spin, the A/B side, and the readout byte number. The matrix rate lookup table is contained in EEPROM, and is thus reloadable if necessary.

4.2. System Processor Unit (SPU) software

Reset Strategy

When power is applied to the system, the 8086 microprocessor (SPU) fetches its reset vector and begins executing its startup code. The startup code performs the following tasks:

Run memory test diagnostics

Locate EEPROM table map

Download 1750 software from EEPROM to EPU instruction and data memories

Start 1750 microprocessors

Initialize hardware and peripheral chips

Initialize RAM memory

Enable interrupts

Transfer to main program

The reset vector and startup code are fixed in PROM memory. Whenever the SPU is reset, the same vector and startup code are fetched. Resets may occur for

several reasons other than power up, and the startup code attempts to distinguish between the various types of resets and tailor the processing accordingly.

Soft Reset

The SPU circuitry includes a watchdog timer that must be cleared by the software on a regular basis. If in case of a malfunction the software fails to do this, the circuitry generates an automatic SPU reset. The processing in this case is designed to resume normal operation with minimum loss of data. If a few basic integrity checks are satisfied, the 1750 microprocessors and the data RAM, which accumulate the scientific data, are assumed to be unaffected. These are among the most radiation tolerant components in the system, which gives this assumption some validity. The interrupt vectors are restored, but the rest of SPU RAM is left untouched, so all state variables are retained across the reset. When the main program is rejoined, normal processing resumes. Soft resets are counted and telemetered. In order to avoid a race that causes continuous soft resets, the software generates a hard reset when the reset counter rolls over from 255 to zero.

Hard Reset

The startup code cannot distinguish between a watchdog timer reset and a commanded reset relay closure. Therefore the latter will normally generate a soft reset as described above. In order to cause a hard reset, a special 'force hard reset' serial command must be sent prior to the relay closure. The startup code detects the presence of this command in the hardware command latches and performs the equivalent of a power up reset. The power up condition itself is distinguished by the presence of a bit latched in the hardware power up detection circuitry, which makes the power up hard reset operation reliable.

ROM Boot

It is possible for the EEPROM contents to be permanently corrupted to disable the microprocessor from correctly performing its hard reset sequence. If such a condition occurs, either through incorrect commanding or component failure, operator action is required to locate the corrupted portion of EEPROM and rewrite it or map around it. A variant of the 'force hard reset' command is the 'ROM boot' command, which directs the microprocessor to avoid using EEPROMs at all during its hard reset. In this configuration, scientific data processing is disabled, but commanding and telemetry are enabled. This allows reloading of the EEPROM tables and corrected operation at the next hard reset.

Table Management

Most of the system's scientific data processing is controlled by code and data tables in EEPROM. The table management system is designed to permit flexible reconfiguration of the instruments with redundant backup reliability. To accommodate the possibility of radiation-induced failure of portions of EEPROM, the tables are not

required to be at fixed addresses within EEPROM memory. Instead, a 'master map' contains pointers to each of the tables in EEPROM, and a 'backup map' contains pointers to backup copies of the same tables. There are default maps in PROM, which can be superseded by maps uploaded into EEPROM. Each table is equipped with an identifying header and checksum. During a hard reset, the master map is located, and each of its table pointers are checked to make sure that there are valid tables at those locations. The table status bits are retained and telemetered. The instrument can continue to operate with missing or corrupted tables, automatically disabling the corresponding functions.

During normal operation, the software checks the primary and backup copies, cycling through all of the tables. If either copy of any table is found to be corrupted, an attempt is made to replace it from the remaining good copy. Successful replacements are noted and telemetered. Unsuccessful replacements cause the corresponding table status bit to be cleared. Operator action is required to move the table to a usable area of EEPROM and update the master map.

Serial Commands

Serial commands are 40 bits long, and are categorized according to spacecraft requirements into major mode, minor mode, load address, and load data commands. ELITE and LEMT use only two major mode commands each, which are associated with reset operations. Minor mode commands contain a 12-bit address and 16-bit data field, allowing modification of many software variables and parameters during instrument operation. Most instrument configuration is performed through load address and load data commands. A table upload begins with a load address command, which informs the microprocessor where to load the table. Each succeeding load data command transmits 32 bits of table data, up to a total of 4K bytes. Tables are generally loaded into EEPROM, where they remain permanently even when instrument power is cycled; however certain temporary reconfigurations may be accomplished by loading directly into RAM.

Telemetry Formatting

A single telemetry buffer is maintained in SPU RAM. This buffer feeds the hardware telemetry FIFO. After the last byte of the buffer is placed in the FIFO, the software can begin to format the buffer for the next Major Frame. The FIFO is 512 bytes deep, and at the normal telemetry rate this provides about 20 s in which the next Major Frame can be prepared. Telemetry formatting does not normally begin just when the buffer is emptied. Instead, the program waits for the next complete spin (a maximum of 3 s) before starting to format the next Major Frame. In this manner the scientific data are accumulated in whole spins. At the normal spacecraft telemetry rate of 92 s per Major Frame, each Major Frame contains either 30 or 31 3-s spins. To support bench testing modes in which the telemetry is accelerated by as much as a factor of 16, the program makes a decision based on the number of spins in the Major Frame to see if it can wait for the spin to

complete or if it should read out the data immediately and forego spin alignment. The 1750 microprocessors are stopped briefly while the accumulated data are read out into RAM. The hardware rates continue counting, but software event analysis is held off during this time. The EPUs are then restarted to accumulate the next Major Frame, while the data are formatted for the telemetry. Telemetry formatting is controlled by a 'program' contained in a small EEPROM table. The program specifies the sequence of packets that are to be assembled to fill the Major Frame. Each telemetry packet contains an identifying header describing its contents. The data analysis software is packet-driven, and does not require the packets in any particular order. Thus the Major Frame contents are reconfigurable if a special need arises.

5. Ground Support Equipment

The Ground Support Equipment (GSE) consisted primarily of a spacecraft simulator, frame capture buffer, and a box which provided 28 V for the instrument low voltage power supply and survival heaters. This box included a current meter, which gave a very useful indication of the first order health of the instrument, and a cumulative runtime meter. LEMT and ELITE/STEP each have their own independent GSE.

5.1. Spacecraft simulator

A spacecraft simulator, in the form of a plug-in board for a personal computer, was designed for testing each instrument prior to delivery to the spacecraft. It provides a telemetry interface, the ability to send serial and pulse commands, and Sun and magnetic field-crossing pulses and corresponding spin clocks, as well as support of passive thermistors and digitization of multiplexed analog voltages. (Passive thermistors are thermistors which can be read by the spacecraft whether the instrument is on or not.) The telemetry data is converted to a serial bit stream which is essentially identical to that coming from the spacecraft; accelerated bit rates are supported in addition to the nominal spacecraft data rates. The current date and time are also included in the telemetry stream in the same format as is used by the spacecraft. Multiple copies of this board made it possible for different instruments to be tested independently.

5.2. Frame capture buffer

A frame capture buffer board, also a plug-in board for a personal computer, was designed to capture telemetry data one Major Frame at a time. The same board is used to capture telemetry data regardless of whether it comes from the spacecraft simulator board, from the Spacecraft Checkout Station during spacecraft integration and test, or from the Operations Control Center after launch. The frame capture

buffer board only captures the bytes which belong to a specific instrument. The information as to which bytes to capture is contained in a format data file in the personal computer. This file is used to program both the spacecraft simulator board and the frame capture buffer board. The captured data can be displayed as it is being acquired and, if desired, archived to disk. Archived data files can be similarly displayed after the fact. The displays are basically of two types. The first of these is frame by frame updates of groups of related quantities all displayed together. The second consists of scatter plots or time history plots which represent intervals much longer than a single Major Frame.

Acronym List

ADC	Analog to Digital Converter
APE-A, APE-B	Alpha Proton Electron telescope systems A and B
CIR	Coronal Interaction Region
CME	Coronal Mass Ejection
DPU	Data Processor Unit
EEPROM	Electronically Erasable Programmable Read Only Memory
ELITE	ELectron Isotope TElescope system
EPU	Event Processing Unit
FET	Field Effect Transistor
FIFO	First In First Out
FIP	First Ionization Potential
GSE	Ground Support Equipment
HVPS	High Voltage Power Supply
IT	Isotope Telescope
LEMT	Low Energy Matrix Telescope
LiD	Lithium Drifted
LLD	Low Level Discriminator
LVPS	Low Voltage Power Supply
MCP	Microchannel Plate
MUX	Multiplexer
PHA	Pulse Height Analyzer
PROM	Programmable Read Only Memory
PSD	Position Sensitive Detector
RAM	Random Access Memory
SEDA	Secondary Electron Detection Assembly
SEU	Single Event Upset
SPU	System Processor Unit
TAC	Time to Amplitude Converter
TOF	Time of Flight
T/H	Track and Hold

Acknowledgements

At the substantial risk of overlooking somebody, we wish to acknowledge the contributions of the following key individuals:

GSE Hardware: Jeff DuMonthier, Bob Smith

Power Supplies: Manuel Florez, Dave Galosky, Bob Kichak, Luan Vo, Edvin Tums

ELITE Enclosure: Frank Shaffer

ELITE Telescopes: Sandy Shuman

LEMT Mechanical Design: Harry Trexel

STEP Mechanical Redesign: Tom James, Mark Sardella

Solid State Detectors: Bill Davis, Greg Delo, Maureen Madden, Karl Heuerman

Thermal Design: Cindy Edgerton, Robert Kidwell

Software: Tom Nolan, Phong Le, Suri Tipparaju, Kristin Wortman

Printed Circuit Board Layout: Phil Goodwin, Marci Holzapfel, Maggie Rilling

Technicians: Mike Barciniak, Mo Beazley, Pat Bent, Greg Delo, Norm Dobson, John Pickett, Ken Simms, Terri Simms, Hank Wats

Others: Bernie Fridovich, Richard Liberman, George Croft, Lisa Kelly, Maxine Windhausen, Robert Joyce, Don Stilwell, Sharon Smith, Marianne Leviton, Ed Werner, Susan Wang, Wendy Nicholas, Joseph Mazur

Support Companies: EER, Ideas, Litton, Martin-Marietta, UNISYS

Project/GSFC Support: Environmental Test, GSFC Code 754, Plating Shop, GSFC Code 752, Quality Assurance, GSFC Code 300

The Support Staff at the following facilities provided outstanding support:

Tandem Van de Graaff Facility at the Brookhaven National Laboratory; Holifield Heavy Ion Research Facility at the Oak Ridge National Laboratory; the Bevalac at the Lawrence Berkeley Laboratories; the National Superconducting Cyclotron Laboratory at Michigan State University.

Surface barrier detectors were provided by EG&G ORTEC. Lithium drifted detectors were provided by Jack Walton of the Lawrence Berkeley Laboratories. Ion-implanted detectors were provided by Micron Semiconductor, Inc. Microchannel plates were provided by Galileo Electro-Optics, Corp.

References

Barbier, L. M., Reames, D. V., and von Rosenvinge, T. T.: 1993, *Proc. XXIII Int. Cosmic Ray Conf., Calgary* **3**, 222.

Miller, J. A. and Viñas, A. F.: 1993, *Astrophys. J.* **412**, 386.

Perkins, M. A., Kristoff, J. J., Mason, G. M., and Sullivan, J. D.: 1969, *Nucl. Inst. Methods* **68**, 149.

Reames, D. V.: 1990, *Astrophys. J. Suppl.* **73**, 235.

Reames, D. V., Meyer, J. P., and von Rosenvinge, T. T.: 1994, *Astrophys. J. Suppl.* **90**, 649.

Reames, D. V., Richardson, I. G., and Barbier, L. M.: 1991, *Astrophys. J. Letters* **382**, L43.

Simpson, J. A. and Garcia-Munoz, M.: 1988, *Space Sci. Rev.* **46**, 205.

Temerin, M. and Roth, I.: 1992, *Astrophys. J.* **391**, L105.
UTMC: 1990a, 'UT1750AR RISC Microprocessor', United Technologies Microelectronics Center (UTMC), Colorado Springs, Colorado, Data Sheet.
UTMC: 1990b, 'UTD-R Gate Array Family', United Technologies Microelectronics Center (UTMC), Colorado Springs, Colorado, Data Sheet.
von Rosenvinge, T. T., Barbier, L. M., and Reames, D. V.: 1993, *Proc. XXIII Int. Cosmic Ray Conf., Calgary* **3**, 400.
Winkert, G.: 1992, IEEE Trans. on Nuc. Sci. 39, 789.